Dexter: A Smart Prosthetic Device for Transradial Amputees

A Major Qualifying Project submitted to the faculty of
Worcester Polytechnic Institute
in partial fulfillment of the requirements for the Degree of Bachelor of Science By

Sienna Mayer

Gabrielle O'Dell

Yesugey Batu Sipka

Date: April 27, 2017

Project Advisors:

Prof. Cagdas Onal, Major Advisor

Prof. Kristen Billiar, Co-Advisor

Prof. William Michalson, Co-Advisor

Abstract

Over 500,000 people in the United States are missing part or all of their lower arm and more than 28 million more are at risk for amputation. Unfortunately, current upper-limb prosthetic devices offer limited functionality and are prohibitively expensive, often ranging from $10,000 to $75,000. Users have been dissatisfied with the current products, with 70% of amputees stating the prosthetic hands limit activities of daily living, and 60% feel the hands limit the amount of work they are able to accomplish. Existing technologies require the user to exert significant cognitive effort to accomplish simple everyday tasks. Users have to be visually aware of their environment to control their prosthetic device and interact with objects, severely inhibiting functional utility and convenience.

To address these challenges, a smart below-elbow prosthetic, called Dexter, was created using sensors and a camera to "feel" its environment and act intelligently. The project involved the design, fabrication, and testing of Dexter as an inexpensive, intuitive, and intelligent alternative to existing prosthetic hands. Dexter can adjust its position, orientation, and grip based on visual and force feedback to detect objects, determine appropriate grasps, and maintain object orientation without the need for extensive user input. After four years of iterative design, this new paradigm of "assistive intelligence" has resulted in an anthropomorphic hand that is capable of autonomously functioning and responding to its environment. In the future, this intelligent hand can be used for advanced research applications and everyday use. Ultimately, the team expects that Dexter will bring about a paradigm shift in prosthetic design.

Acknowledgements

First, our team would like to thank our project advisor, Professor Cagdas Onal, for his technical insight and support, and the project co-advisors, Professor Kristen Billiar and Professor William Michalson, for providing necessary tips and guidance as needed. The success of this project was greatly influenced by the advisors' guidance along the course of the project.

The team would also like to give a special thanks to David Croke from the WPI Office of Human Resources for his constant presence throughout the year. He provided critical tips that kept the team grounded and considerate of the business and future human interaction aspects of this project.

Finally, the team would like to thank Aditya Gupta, a WPI Masters Student, and Selim Ozel, a WPI PhD Candidate, for their support throughout the year. Without Aditya's contributions, the camera and object recognition used in this device would not have been possible. Additionally, without the constant input from Selim, the team would not have been as successful in the technical revisions necessary to create a fully functioning device.

Copyright Note

Contents

Table of Figures

Table of Tables

1. Introduction

One in every 190 Americans currently live without one or more of their limbs, with the number expected to double by the year 2050 (Ziegler-Graham, K. et al., 2008). A number of diseases have created a growing percentage of Americans with limb loss, with nearly 28 million people at risk for amputation (Limb Loss Statistics, n.d.). Although lower limb amputations are more common, there is a growing need for well-designed upper limb prosthetics to help amputees successfully complete tasks during daily living. This project focuses on the needs of over 500,000 Americans with transradial (below-the-elbow) limb loss (Zieger-Graham, K et al., 2008).

Despite the growing need, there are few affordable, highly-functional prosthetic hands on the market. Current devices lack functionality, leaving 70% of upper-limb amputees with a prosthetic device saying that their device still limits their ability to complete daily tasks (Inspector General, 2012). Most commercially available prosthetic devices cost over $10,000, with some brands as high as $75,000 (Michelangelo Brochure & BeBionic3, 2013). With the growing popularity of 3D printing, new light-weight, low-cost devices are emerging on the market. These prosthetics, while cheaper and more customizable than others, are currently far less durable and strong (AdaV1.0, 2016).

The lack of low-cost, high-functioning upper limb prosthetics has left a gap in the market. Amputees must make a choice between a low-cost, low-functioning device, such as hooks, or an expensive, highly-functional prosthetic. While the high-end devices offer an anthropomorphic profile, they are often more complex to use, causing some amputees to return to the low-cost hooks or non-functional cosmetic prostheses.

There are devices that have integrated sensors, but most are myoelectric and can only detect what tendons the user is trying to move and control the hand accordingly. No prosthesis currently exists that can sense its environment to autonomously locate objects and grasp them with appropriate force. This project focuses on the design and development of a smart prosthetic device that can assist the user with minimal input.

After four years of previous project iterations, the team will build upon findings of past teams to produce a final, fully functioning device. Analysis of past years led to the decisions to keep the finger and thumb design. All other mechanical, electrical, and software components were completely redesigned to create the final device. This prosthetic will utilize 3D imagery and object classification to locate the desired object and move the hand into the correct orientation to grasp. With one input from the user, the hand will grasp the object, and maintain the correct force and orientation to move the object without crushing, dropping, or spilling the contents.

2. Background

Background research was conducted on the following topics to better understand how to address the current market needs: anatomy, current prosthetics, additive manufacturing, tactile sensing, and visual object recognition. This research was combined with the findings and approaches conducted by previous versions of this MQP. This information helps to outline the needs of the user, the gap in the market, and technologies that could make Dexter innovative.

2.1 Anatomy

The human hand is a complex structure comprising bones, muscles, tendons, and ligaments. Carpals make up the compound wrist joint, metacarpals create the palm, and proximal, intermediate, and distal phalanges make up each finger. The thumb is the one exception, having only a proximal and distal phalange. Thirty-four muscles within the hand and forearm control the movement of this bony structure and create twenty-two degrees of freedom (DOF) in total: each finger and the thumb have three flexion and one abduction and two more between the metacarpals of digits four and five to allow palm curling (Casley, S et al., 2014). These structures and their corresponding degrees of freedom are shown in Figure 1 below.

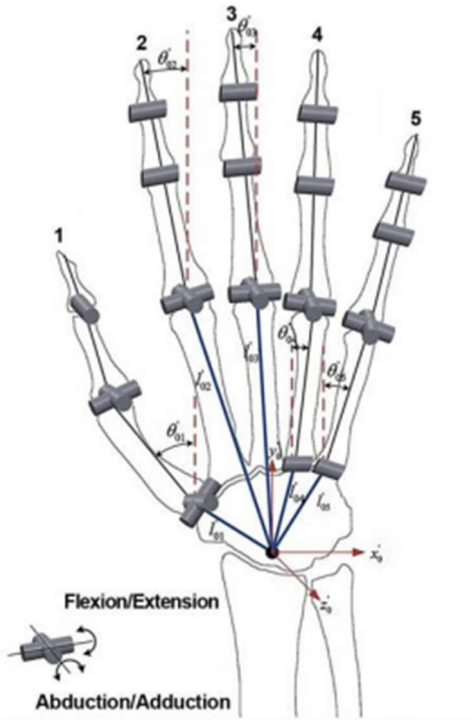

Figure 1: Hand joint diagram and degrees of freedom (Casley, S. et al., 2014).

Flexion/extension and abduction/adduction are the two possible finger movements (DOF) as a result of muscle contraction and relaxation. There are no muscles within the fingers. Instead, tendons connect the phalanges to muscles in the palm and forearm. Palmar muscles are intrinsic and include the thenar which powers the thumb, hyposthenia which powers the little finger, dorsal and palmar interossei which control the middle three fingers, and the lumbrical muscle which flexes the metacarpal joints. Muscles located in the forearm are extrinsic and are used for finger flexion and extension (Casley, S. et al., 2014).

By controlling these muscles and finger movements, different prehension patterns are possible. Figure 2 below highlights six of the most important types of prehension, or grasps, for daily living. Jaw Chuck, more commonly known as tripod grasp, tip grasps, and lateral grasps are the three most commonly used (Billock, 1986). In cases when an object needs to be picked up tip grasps will occur 71% of the time and in cases of holding an object for longer term use tripod grasp is used 88% of the time (Billock, 1986).

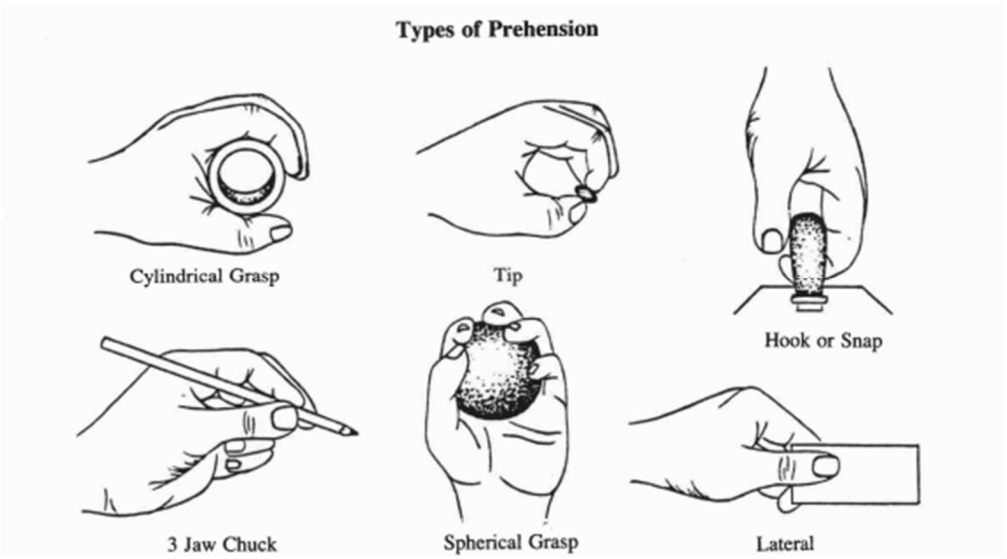

Figure 2: Grasps commonly used for activities of daily living (Billock, 1986).

Proper anatomical sizing of the hand is desirable for achieving an anthropomorphic device. A study published in the *International Journal of Morphology* provides useful data on the proper ratios for finger sizing. X-rays of 66 adults within the ages of 19 to 78 were taken and analyzed to create accurate proportions of the human hand (Buryanov, 2010). Figure 3 shows an example of the x-rays taken and measurements used to populate

Figure 3: Bone labeling schematic corresponding to Table 1 (Buryanov, 2010).

Table 1: Phalange, metacarpal, and soft tissue lengths (Buryanov, 2010).

Finger	tip – soft tissues of the tip of the distal phalanx (mm)	pd–distal phalanx (mm)	pm–medial phalanx (mm)	pp–proximal phalanx (mm)	m–metacarpal (mm)
I	5.67±0.61	21.67±1.60		31.57±3.13	46.22±3.94
II	3.84±0.59	15.82±2.26	22.38±2.51	39.78±4.94	68.12±6.27
III	3.95±0.61	17.40±1.85	26.33±3.00	44.63±3.81	64.60±5.38
IV	3.95±0.60	17.30±2.22	25.65±3.29	41.37±3.87	58.00±5.06
V	3.73±0.62	15.96±2.45	18.11±2.54	32.74±2.77	53.69±4.36

Values are presented as arithmetic mean ± SD.

2.2 Prosthetics

Need for Prosthetic Limbs

One in every 190 Americans lives with limb loss, however, this number is estimated to double by 2050 (Ziegler-Graham, K. et al., 2008). Every year in the United States, 500 amputations take place per day, for nearly 185,000 amputations a year (Limb Loss Statistics, n.d.). In 2005, 1.6 million people suffered from a loss of limb. This is caused by a number of factors, including amputation and birth defects. Of these 1.6 million, the causes for amputation were dysvascular disease (846,000), trauma (704,000), diabetes (592,000), and cancer (18,000) (Ziegler-Graham, K. et al., 2008).

The Amputee Coalition of America has estimated that an additional 28 million people are at risk of amputation due to the rise in diabetes nationwide (Limb Loss Statistics, n.d.). The number of people affected by limb loss is expected to increase to 3.6 million by 2050 (Ziegler-Graham, K., et al., 2008).

In 2005, 541,000 people in the United States suffered from upper limb loss. The data, as shown in

Table 2, was split into two categories: minor and major limb loss. Minor loss includes the loss of fingers, hand, and forearm. Major limb loss constitutes any amputation or loss of limb above the elbow. The study found that 500,000 people suffered from minor loss and 41,000 has major loss of limb (Ziegler-Graham, K. et al, 2008).

Table 2: Estimates of Limb Loss in the 2005 in the United States, Measured in Thousands (Ziegler-Graham, K. et al, 2008).

		Lower Limb		Upper Limb	
Etiology	Total	Major	Minor	Major	Minor
All etiologies	1568	623	404	41	500
Dysvascular disease: total	846	504	302	5	34
Dysvascular disease with comorbidity of diabetes	592	359	212	3	19
Trauma	704	106	101	34	464
Cancer	18	13	1	2	1

NOTE. Totals may not equal sum because of rounding. Cases missing information regarding level (34%) were assigned to specific level according to distribution.

This project focuses on the development of a transradial, or below-the-elbow, prosthesis. This is an area with a growing need for new, better prosthetic devices, as seen in a 2011 study by the Veteran's Affairs, which states that the majority of amputees were dissatisfied with the current products on the market. Approximately 70% of amputees felt that current hands limited their day-to-day activities, 60% said the hands limited the amount of work they could accomplish, and 45% said they interfered with working in general (Inspector General, 2012). While current devices help in day-to-day life, the dissatisfaction by users show there is still a need for an affordable and functional prosthetic hand.

Non-Anthropomorphic Devices

Non-anthropomorphic, or non-human-like, prosthetic hands can be categorized into hooks and prehensors (Bowers, 2014). These devices are generally more rugged and meant for achieving basic activities of daily living. Split-hooks are two hooks joined by a hinged spring that allow a user to grasp objects when a force is applied to squeeze the hooks together. Hooks are often chosen over other terminal devices because of their high precision and dexterity paired with a low weight. A hook prosthesis weighs approximately one third of that of a full hand (Billock, 1986). Prehensors, which have been developed to be more functional than hooks, are made up of a hinged thumb like component and forefinger like component that work together to grasp objects (Bowers, 2014). Although these devices can be electrically powered, they are usually mechanically-driven by body movements and cable systems or switches.

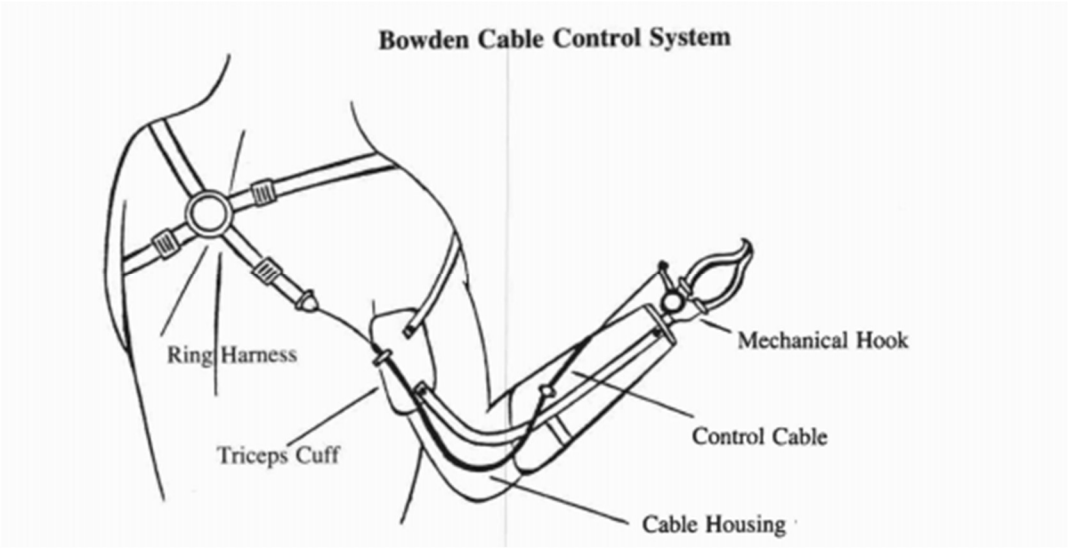

Figure 4: Mechanics of a body powered cable-harness system (Billock, 1986).

Cable-harness systems, shown above in Figure 4, use body motions of flexion and abduction to cause tension or relaxation in the control cable which in turn powers the terminal device. These devices can be voluntary opening or closing (normally closed or open, respectively) and using the cable system up to 44.5 N of prehensor force can be achieved with voluntary opening (Billock, 1986). Voluntary closing terminal devices are devices that must have an applied force to close. In comparison to voluntary opening devices, which require a force to open the device, voluntary closing is more intuitive and easy to use since the user receives tension feedback through the cables, allowing them to feel and control their grip as needed (Bowers, 2014). Switches are another option to cause the opening/closing and can be a toggle, rocker, button, or pulled mechanism (Billock, 1986).

The AxonHook by Ottobock and GRIP 5 Evolution Prehensor by TRS are two examples of high function non-anthropometric terminal devices on the market. The AxonHook, Figure 5, was designed as a supplemental wrist attachment to users of the Michelangelo Hand. This product is durable, but still provides high levels of feedback, finite control, and has a grip force of up to 111 N (25 lbs), making the attachment beneficial for activities of daily living (AxonHand). The GRIP 5 Evolution Prehensor, Figure 5, is a voluntary closing device that has a large opening span of 7.8 cm and can be used for precision work (Adult Grip 5). TRS as a company specializes in various non-anthropomorphic upper arm terminal devices for a variety of sports and recreation activities that allow for high performance in areas such as basketball

or kayaking. These devices are beneficial since they allow for a cheap and effective solution for users who want to maintain their active lifestyle.

Figure 5: (Left) Ottobock AxonHand © Ottobock (AxonHand). (Right) TRS Grip 5 Evolution Prehensor © TRS (Adult Grip 5).

The nature of body-powered non-anthropomorphic devices makes them cheaper, lighter, and easier to repair. Their cable-driven nature also provides feedback to the body. However, these devices also require the user to have a high physical ability and look more like a tool than a human hand (Bowers. 2014).

Anthropomorphic Devices

For an upper-limb prosthesis to look and act in a way similar to a human hand, anthropomorphic prostheses - or artificial hands - are necessary. These devices are advantageous due to their increased grip force and grasping abilities and because they do not require the user to wear a harness or cable since they are battery powered and generally controlled by myoelectric signals, pressures, or strain gauges (Bowers, 2014). These features come at a higher price, are heavier, and make the prosthetic device dependent upon battery life. There are a variety of companies and prosthetic hand designs available. However, the Michelangelo Hand, Ada Hand, i-limb ultra, and BeBionic are four of the leading prosthetic hands.

The Michelangelo Hand (Figure 6) by Ottobock is a myoelectric powered device. The hand has two drivers, the first being for the grip movement and grip force and the second being for the thumb drive and changing thumb position. In the main drive, only the thumb, index finger, and middle finger are actively driven. The ring and little fingers both follow passively. With this configuration, seven different grips are possible: lateral pinch, lateral power, finger abduction/adduction, tripod pinch, opposition power, open palm, and neutral hand (which is the resting position when the hand is not in use). In opposition grips the maximum force is 70 N, lateral grips are 60 N, and the neutral force is 15 N. To increase the anthropomorphic properties of the hand, the fingertips are made of a soft material and a skin-like glove can be placed over the hand - making both the visual and physical properties of the prosthetic more like that of a human hand. However, even with this glove the hand is not suitable for applications such as swimming or showering where there is prolonged exposure to water (Michelangelo Brochure).

Figure 6: Michelangelo Hand © Ottobock (Michelangelo Brochure).

The wrist is another high point in the design of the Michelangelo Hand. Flexion and extension (75 and 45 degrees respectively) and a full 360 degrees of rotation are possible. As the wrist rotates, it is possible for the user to lock the wrist in place at 15 degree increments depending upon the application. Ease of use continues with the simplistic charging mechanism in place. Buttons on the device can be used to turn the prosthetic on/off and the 11.1 V lithium battery in the arm can run for ~1,500 mAh. When the battery dies, the user must simply connect a magnetic charger and watch on the LED display for the battery capacity to rise (Michelangelo Brochure).

The i-limb ultra by Touch Bionics (Figure 7) is another device that can be controlled by myoelectric sensors or by a quick grip phone app. Each finger on the hand is driven, however the thumb is not driven for rotation, instead the user must manually rotate the thumb as desired. Fourteen grips are possible with this hand: four precision pinches, four tripod grips, and six additional grasps. To move from an open hand position into a full grip only takes 1.2 seconds and slipping is prevented using an auto-grasp feature. Each finger can hold a static load of 313.8 N. Multiple wrist attachments are available for use with Touch Bionics prosthetic hands, the best being the multi-flex wrist which allows for spring loaded flexion, extension, and deviation in the passive mode and locked positions of 30 degrees palmar or dorsiflexion. Device coatings and a return to neutral hand position are also features of the i-limb devices to make the prosthesis more realistic. (i-limb ultra, 2013).

Figure 7: i-limb ultra by Touch Bionics © Touch Bionics Inc. (i-limb ultra, 2013).

BeBionic (Figure 8) is another myoelectric hand that's claimed to be 'the world's most advanced prosthetic hand' by Steeper. This device features individually driven fingers that can hold up to 245 N alone or 441 N when used in a hook grip. Like other devices this hand has fourteen grip patterns based on the thumb opposition state. There are four opposed thumb grips including power and index grips, four non-opposed grips such as column and key grips, and six additional grips like a relax hand and precision grips. Some of the features in this hand that make it more advanced are the soft controls within the hand. Microprocessors that monitor the position of each finger make precise motions and speed control possible, so the hand movements are precise and reliable enough to easily hold delicate objects. The device can also automatically sense if an object is not being gripped tight enough and will auto grip and adjust to prevent items from slipping. These features paired with the bebalance software allows for customization to optimize the hands performance. Anthropomorphic features of this hand are furthered by soft fingertips which make the hand feel more realistic while maximizing surface area to increase the stability of objects being gripped and gloves are once again possible to cover the hand (BeBionic3, 2013).

Figure 8: BeBionic by Steeper © Steeper (BeBionic3, 2013).

Four wrist options with varying ranges of motion are also offered for use with the BeBionic hand. Some simply allow for passive rotation while others allow for wrist locking at 30 degrees of flexion or extension. The Multi-Flex wrist is the most advanced option offered. Passive motion in every direction in addition to the ability to lock at 30 degrees of flexion and extension makes the wrist more useful. This wrist is also the most robust option and was designed with a high compliance, making it capable of absorbing shock or external torque. (BeBionic3, 2013)

The Ada Hand (Figure 9) by OpenBionics is another myoelectric hand, but one that represents a more recent direction for prosthetic devices. The Ada Hand is completely open source and made largely from 3D printed parts. This device can be bought online and assembled by anyone in under an hour using simple tools. Each finger in the hand is driven and movement is controlled by strings in tension that reach throughout the entire finger and connect to the motors in the palm. Five grips with varying weight limits are possible with the Ada Hand: fist grip - 9.8 N, palm - 49 N, tripod - 6.9 N, pinch - 3.9 N, and pointing.

Although five degrees of freedom are possible with this device, compared to the other prosthetic hands discussed this simplistic hand lacks qualities and features of a high functioning hand. (AdaV1.0, 2016)

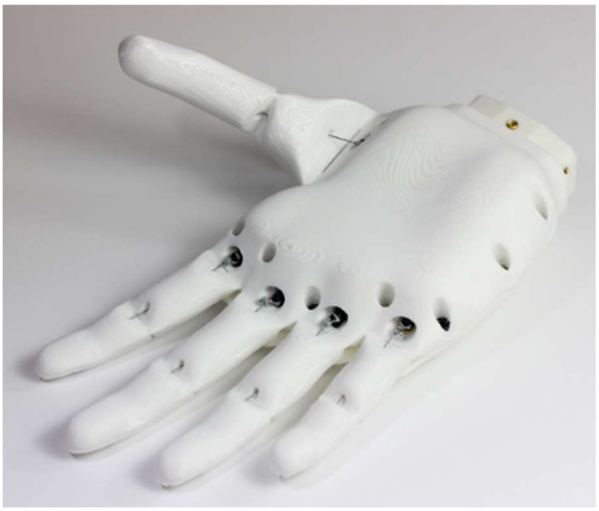

Figure 9: Ada Hand by Open Bionics © Open Bionics (AdaV1.0, 2016).

Overall, there are a variety of high functioning prosthetic hands on the market. However, as a general trend, the higher functioning the device, the higher the cost, as shown in Table 3. When comparing the Michelangelo, i-limb ultra, and BeBionic hands certain anthropomorphic traits are constant throughout and can be considered normal for prosthetic hands on the market. These things include a neutral hand position, flesh colored glove coverings, and usually softer fingertips. Visually, the design of these three hands are similar and they have a battery life in the same range; making the sensing, grip force, and speed characteristics that set each hand apart. BeBionic is currently the leader in these categories, with a fast speed to closure, many precision sensors, and the highest possible grip force. However, this device is also the heaviest one of all and comes at a price of over $10,000. The Ada Hand fits into the prosthetic space as a competitor because of its low price, under $1,000. Although a tradeoff for this type of design is functionality. The Ada hand does have five grip patterns, only two fewer than some of the more expensive alternatives, which is largely due to the non-rotational thumb. Maximum load is another disadvantage to this hand since it can only hold up to 49 N. Overall, this device can be used for activities of daily living, however the stark differences between affordability and function show that there is still a need for an affordable and highly-functional prosthetic hand that is positioned between these two extremes.

Table 3: Summary of Some Prosthetic Devices & Hands on the Market

Hand	Price ($)*	# Grips	Weight (g)	Max Grip Force (N)**	Speed	Battery Life (mAh)
Axon Hook	15,000	N/A	N/A	111	N/A	N/A
Grip 5 Prehensor	1,200	N/A	255	N/A	N/A	N/A
Michelangelo	75,000	7	420	70	325 mm/s	1500
I-limb ultra	17,000	14	500	100	1.2 s	2000
BeBionic	11,000	14	700	140	1 s	2200
Ada	700	5	380	49	N/A	N/A

*in some cases estimates based upon research, **for power grip

Connection to Residual Limb

Prosthetic devices connect to the user's body through a socket. Sockets are made by plaster casting or laser scanning the residual limb and then iteratively fitted until it is anatomically contoured to the user's body and pressure points or areas where rubbing might occur are minimized. Users will typically place some type of liner or compression sock over the residual limb underneath the socket for added comfort. Next, the socket is placed over the limb, and the prosthetic device is attached to the end of the socket.

2.3 Manufacturing

Additive manufacturing provides a means of creating a light-weight, low-cost prosthetic. This manufacturing method is the most cost-efficient way of producing and testing a prosthetic hand to meet the goals and objectives outlined for this project. Additive manufacturing (AM) is the process of systematically building an object layer-by-layer to create a 3D object based on a CAD file. This manufacturing method is beneficial compared to conventional methods due to the customization and decreased cost per part when producing a low quantity of a customizable part. As quantities needed of a standard part increase, more standardized manufacturing methods, such as injection molding, may become more cost effective; however, in these early developmental stages of a custom prosthesis, additive manufacturing provides the most cost effective method of manufacturing. A variety of additive manufacturing techniques exist, so the chosen method can be determined based on the desired outcome. Plastic, composites, paper, metal, and wax are commonly used materials in additive manufacturing. Since this project requires a sturdy, but lightweight design, we focus on plastics.

Plastic additive manufacturing can be achieved through a variety of methods:

- Vat photopolymerization: a vat of a resin polymer is cured with laser, projector, or LED light, the final print is then lifted from the resin. Stereolithography (SLA), which uses a laser, is the most common curing method.
- Material extrusion: a thermoplastic is injected through a heated nozzle and deposited systematically to create the desired model. This fused deposition modeling (FDM) is the method of most commercial 3D printers.
- Material jetting (MJ): droplets of a cross-link polymer are jetted and cured with UV light.
- Powder bed fusion: selective laser sintering (SLS) is the most common powder fusion method where a bed of powder fused with laser until the model is complete.

When choosing a method, there are certain tradeoffs that must be considered. Print time, strength, layer height, and cost are just a few of the main considerations when choosing a printer and print parameters. These parameters are also all interconnected. For instance, a smaller layer height will require a longer build time, but results in a much smoother print and a higher infill will increase print strength, but also will increase build time. A summary of different considerations and printing methods is shown in **Error! Reference source not found.** below.

Table 4: Additive Manufacturing Consideration (Murphy).

	SLA	SLS	Poly-Jet	FDM/FFF	Binder Jetting	CNC	Injection Molding	Forming	Joining
Cost- Low Volume	✓	✓	✓	✓	✓	–	✗	✗	✗
Cost- High Volume	✗	✗	✗	✗	✗	✗	✓	✓	–
Lead Time	✓	✓	✓	✓	✓	✓	✗	✗	✗
Material Selection	–	–	–	–	✗	✓	✓	✓	✓
Surface Finish	–	–	–	✗	✗	✓	✓	✓	✓
Tolerance	✓	–	✓	✗	✗	✓	✓	✓	✓
Integrated Assembly	✓	✓	✓	✓	✓	✗	✗	✗	✗
Complexity	✓	✓	✓	✓	✓	–	–	✗	✗
Customizability	✓	✓	✓	✓	✓	✓	✗	✗	✗

✓ is good, – is fair, ✗ is poor

Resolution vs. cost is one of the largest tradeoffs when choosing a method; the better the resolution the higher the cost. The current commercial market for AM is largely focused on FDM 3D printing. These printers take up the least amount of space, allow for ease of material customization, and are the cheapest. The largest trade-off with FDM is the surface finish and overall model strength. Since FDM prints are held together by hot layers of plastic cooling in a desired orientation, these prints have visible layers and a lower strength than printing methods that use lasers to bind the material. However, infill density and pattern in addition to layer height can be controlled to improve the overall finish and strength of the product - making this method the best suited for manufacturing anthropomorphic prosthetics at a low cost.

2.4 Past Iteration by WPI Teams

Human Hand Prosthesis (2012): Paul Ventimiglia

One of the inspirations for this project is the work of Paul Ventimiglia and his paper “Design of a Human Hand Prosthesis,” which was completed as an MQP in 2012. This report created the basis for the finger design and actuation. Ventimiglia’s design broke the finger into two separate joints, instead of the three of a real hand. These joints were connected at the middle knuckle of the finger by a pin, as can be seen in Figure 10.

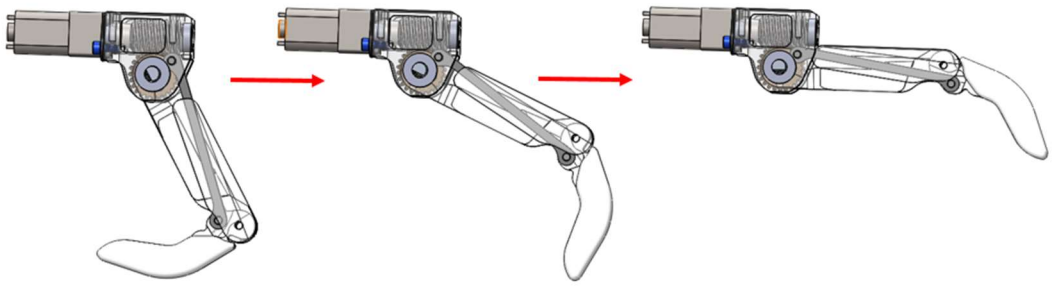

Figure 10: Full Range of Motion of the Finger

The finger was actuated using worm gears at the base of the finger in the "knuckle," as seen in Figure 11. This design allowed for 110 degrees range of motion for each finger, which was monitored by a potentiometer attached to the knuckle.

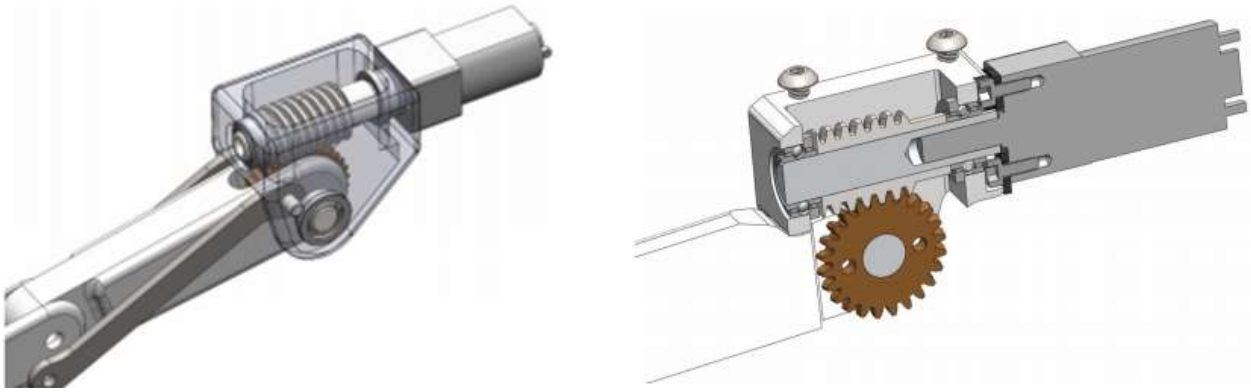

Figure 11: (Left) Worm gear knuckle design and (right) cross sectional view of knuckle design.

The exploded view of the full finger assembly can be seen in Figure 12 below. This knuckle design was used for two of the three previous versions of the smart prosthetic hand. However, the potentiometer was not securely placed on the knuckle. There were no screws or pins holding the potentiometer to the side of the knuckle. The design relied on either glue or force from the knuckles to secure the potentiometer. This posed problematic when the design was prototyped by Frankenhand (2016). Despite this flaw, the knuckle design was very sophisticated and aesthetically pleasing.

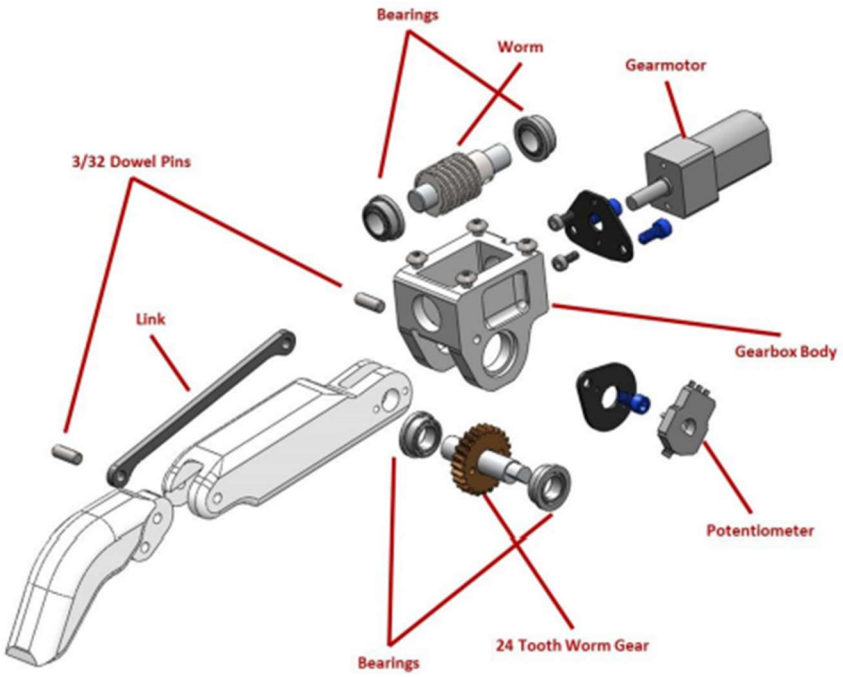

Figure 12: Exploded View of Finger Assembly

The thumb design of this hand is also utilized for later iterations of the project. The two rotations were achieved with a compound gearbox, as seen in Figure 13. The entire assembly is set at a 15-degree angle to the four fingers, making for a more natural, human-like grasp of objects.

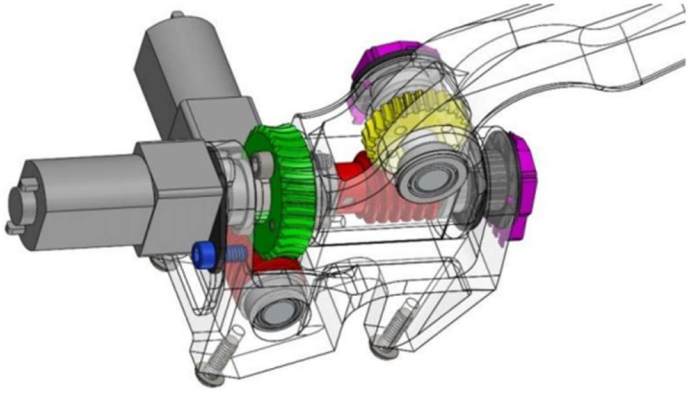

Figure 13: Compound Gearbox for Thumb Mechanism

The yellow and red gears shown in this figure create the same movement used by the individual fingers. The 30-tooth green gear drives the thumb roll, which gives the thumb one more degree of freedom over the other fingers. The exploded view of the thumb assembly is shown in Figure 14.

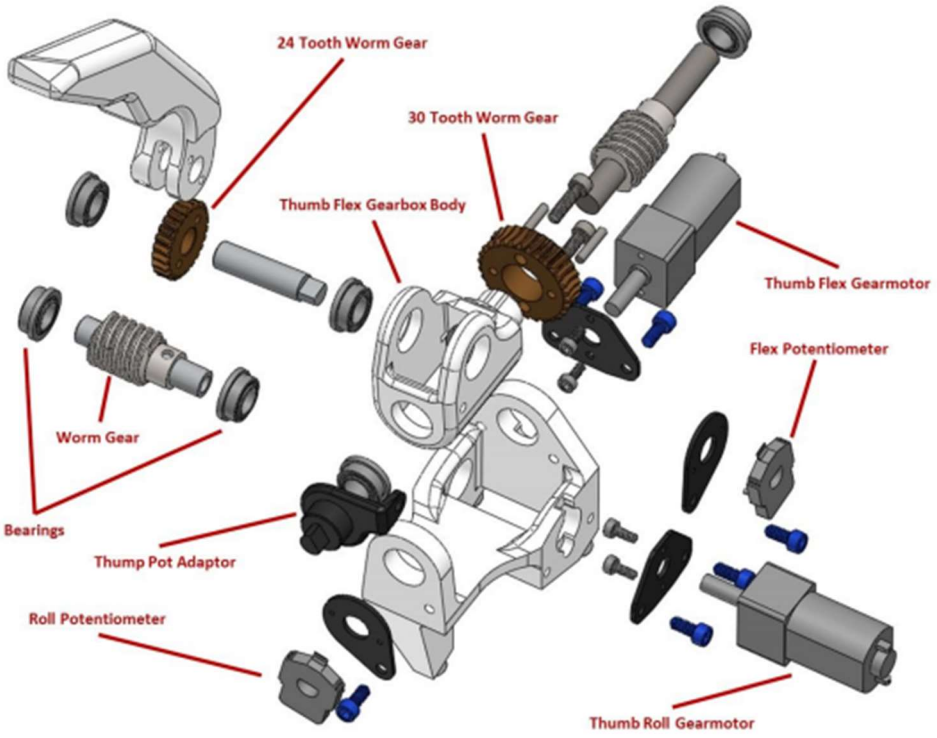

Figure 14: Exploded View of Thumb Assembly

The final market cost for this hand was set at $2,933 (Ventimiglia, P., 2012). This is far cheaper than some of the alternative hands, but over $2,000 more expensive than the Ada Hand. While Ventimiglia's design had increased functionality over other marketed prosthetic limbs, the final design was bulky and untested.

IRIS Hand (2014)

In 2014, an anthropomorphic hand prosthesis with autonomous object recognition was created (Casley, S. et al., 2014). Dubbed the IRIS Hand, this design featured similar mechanisms to Ventimiglia, though it did not derive from his design. This prosthetic hand had linkage-actuated fingers, driven by spring cables, emulating the movement of tendons in the human hand. The spring mechanism for actuating the fingers is illustrated in Figure 15. This series elastic actuation was highly effective, but the spools and motors took up valuable space inside of the forearm.

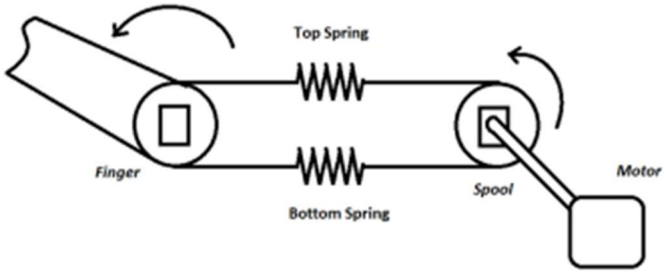

Figure 15: Elastic Actuation Illustration for IRIS Finger (Casley, S. et al., 2014)

Each finger could move independently and was sized per the average size of an adult male. The final version of the finger design, taken from the IRIS Hand report, can be seen in Figure 16. This finger mechanism had a greater range of motion (Figure 17) than Ventimiglia's design.

Figure 16: CAD Model of IRIS Finger Design (Casley, S. et al., 2014).

Figure 17: Full Range of Motion of IRIS Finger (Casley, S. et al., 2014).

In testing, the hand was successfully able to grasp a cube, cylinder, and sphere based on image processing. The hand also had limited success identifying AR tags placed on objects. However, the lower accuracy of identifying the AR tags made this identification process less successful.

The device cost $1,800, which was much lower than traditional prosthetic devices but higher than the cheap 3D printed alternatives. Figure 18 and Figure 19 show the final CAD rendering and the prototype, respectively.

Figure 18: CAD Rendering of IRIS Hand (Casley, S. et al., 2014).

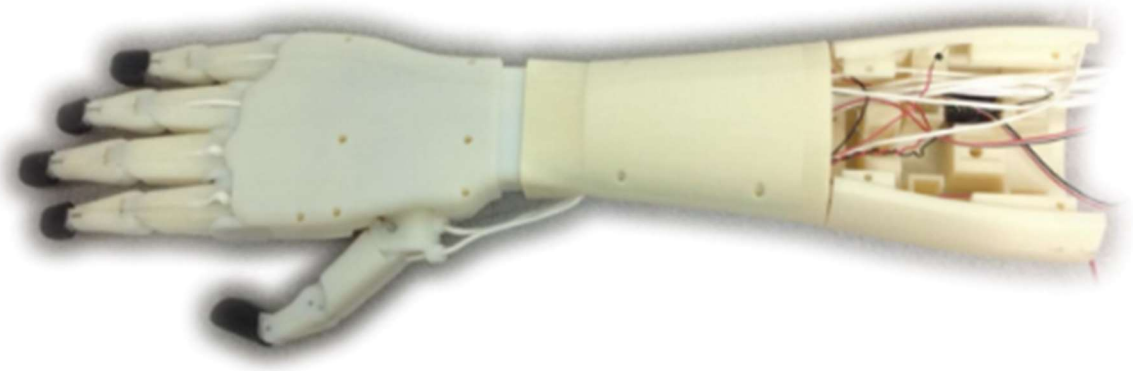

Figure 19: Top View of Full IRIS Hand Prosthetic (Casley, S. et al., 2014).

This device received high praise and won first place in Intel Cornell Cup and the WPI Provost Award in 2014. Despite the success in testing, the IRIS Hand did have a few drawbacks. The arm did not have a self-contained battery and was not fully tested for autonomous movement or grasping with a single user input (Casley, S. et al., 2014). These factors led to the extension of the project for another year.

VIPeR Arm (2015)

The VIPeR Arm was created through the modification of the IRIS Hand in 2015. This design can be seen in Figure 20 below. This version of a smart prosthetic utilized most of the IRIS Hand mechanisms, but with the addition of wrist movements (Edwards, R. et al., 2015).

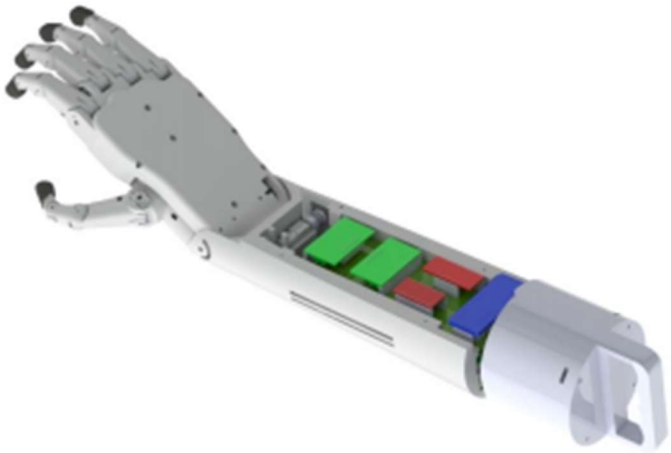

Figure 20: CAD Rendering of VIPeR Arm with Handle for Testing (Edwards, R. et al., 2015).

This design used the same finger linkages, but modified the base of the finger to work with a bevel gear instead of the spring-actuated cable of the IRIS Hand. The use of a gear instead of the original elastic actuation greatly increased the available space within the forearm for other electronic components. The gear also restricted back-driving when the fingers were gripping an object. This new finger (Figure 21) measured force exerted by monitoring the spike in current in each finger's driver motor. The thumb was also redesigned to accommodate the new gearing system. The VIPeR team also made each finger the same size to make the hand modular and easier to repair, as one finger could be easily switched out for any malfunctioning finger, excluding the thumb.

Figure 21: CAD Model for Redesigned Gear-Driven Finger (Edwards, R. et al., 2015).

The wrist had two degrees of freedom. The first was operated using a belt and pulley system that created a pitch motion. The second degree of freedom, roll, was achieved by powering a driver motor to rotate the forearm to the desired angle, which was measured using a potentiometer.

This design had a number of small problems, including the finger sensing and wrist movements. The method of monitoring for current spikes in the motors ended up drawing too much current, as it needed enough to get an accurate or meaningful torque reading. The project team recommended using a tactile force sensor to get a more accurate reading. There were also several problems with actuation in the final design. The belt in the wrist was too loose, resulting in an inaccuracy of up to 40 degrees, and the large number of wires connecting the palm to the forearm limited the amount of achievable movement. The bevel gears in the fingers also allowed for too much slack in the movement, as they were not attached to

the finger itself (Edwards, R. et al., 2015). The project was extended another year to account for these problems and recommendations.

Frankenhand (2016)

All three of the aforementioned projects were combined to create the Frankenhand (Figure 22), which was completed in April 2016 (Merlin, M. & Sullivan, K., 2016). The fingers from Ventimiglia's design were used, but the tip of each finger was widened slightly to make room for force sensors, rather than the electrical current sensing method used in the previous year.

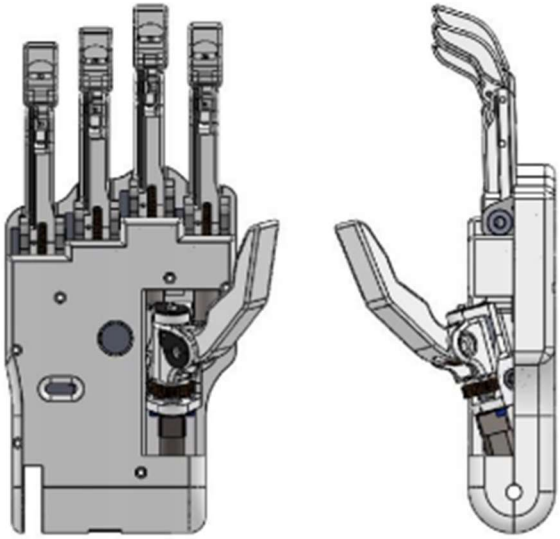

Figure 22: Final CAD Design of Frankenhand (Merlin, M. & Sullivan, K., 2016).

The thumb was modified slightly to achieve roll using two motors: one that rotated the thumb laterally, and another to curl the finger. An illustration of the possible rotations for the new thumb design is shown in Figure 23.

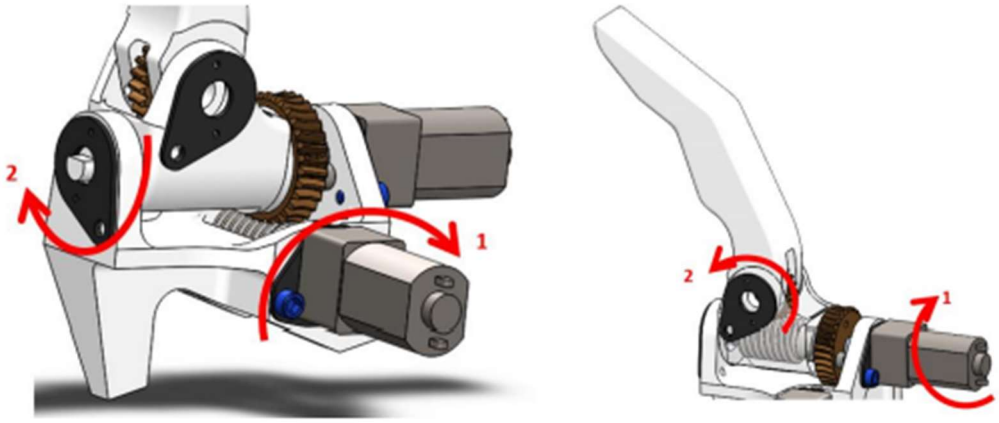

Figure 23: Illustration of Thumb Rotation on Frankenhand

The finger knuckles were taken directly from the previous design, leading to problems with the attachment of the potentiometer. The force fit was not strong enough to keep the potentiometer in place, so the component was glued to the side of the knuckle. The screws used to attach the finger to the shaft stripped during use, resulting in a lack of trackable rotation. This posed a problem when the finger moved, as there was no way of knowing the finger rotation angles accurately, leading to problems when grasping.

The hand was successfully able to power grasp and hold a mug, however, precision grasps were too difficult to complete reliably. Tested grasps were all done manually, as none of the pre-set positions for autonomous movement were implemented. The force sensors were not tested enough to ensure the grip of an object is consistent while the hand is moved around or that the hand maintains enough force to hold an object (Merlin, M., Sullivan, K. 2016). This lack of sufficient testing and data led to the extension of the project for one final year.

2.5 Tactile Sensing

A big problem in prosthetics is the inability to imitate the "feeling" aspect of a real limb. With the rapid evolution of technology, the capability of recreating the feeling of touching an object can now be applied to the field of prosthetic devices.

Most prosthetic hands in the market have a predetermined number of grasps and integrated sensors to achieve human-like, natural movements. These sensors transmit signals from the limb to the prosthesis to initiate the grasp or even control the hand. Despite this, sensing in prosthetics has not been fully developed. Most hands on the market do not have sensors that interact with the environment outside of the hand, and are therefore unable to get feedback from the environment or sense the object the user if touching. Most feedback is thus through user commands. The user visually estimates what they are trying to grasp, how far the object is from the hand, and actively commands every motion of the prosthetic device accordingly. Sensing the environment would be greatly beneficial to a prosthetic hand. Not only would sensing increase the precision of the device, it also makes everyday tasks easier for the user, as they don't have to visually confirm the hand is touching the object every time they command the hand to grasp. Figure 24 shows the steps a smart prosthetic hand must go through to pick up an object.

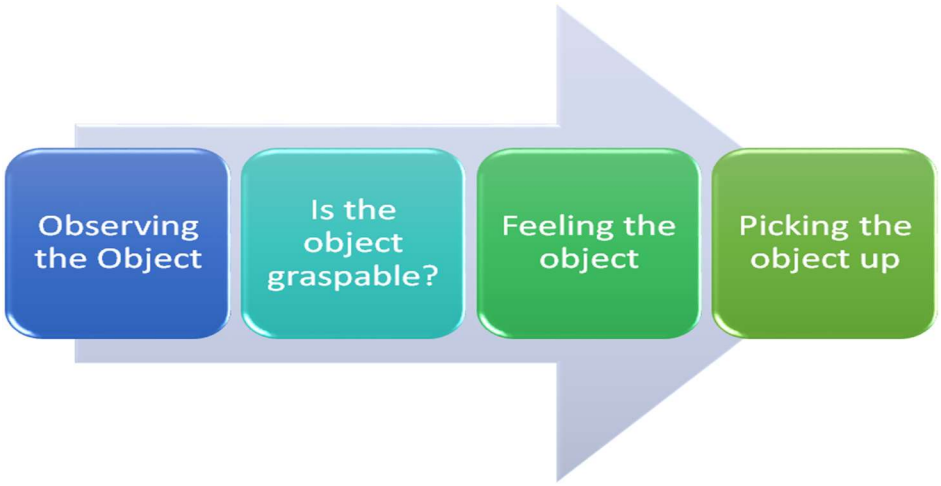

Figure 24: Steps in Recognizing and Picking Up Objects in Environment

Tactile sensing can be achieved in a number of ways; however, this report focuses on the sensing of force and current. The ability to sense the amount of force applied to critical parts of the hand, fingertips for example, is a very powerful tool for a smart prosthetic device. Force is measured with mechanical or resistance-based force sensors. These sensors convert mechanical load into an electrical signal. As more force is applied to the sensor, the output value increases.

Another form of sensing is current sensing. This can be done directly by placing a shunt resistor in series with the motor driver circuit and measuring the voltage across it. Current sensing can also be done indirectly by placing a coil around the current-carrying conductor and measuring the voltage across the coil. The induced voltage in both cases is proportional to the current flowing through the system (Semig, P., & Wells, C., 2012).

Adding sensing to a prosthetic device could vastly expand the number of objects it could successfully pick up. Sensing gives the hand the ability to hold a Styrofoam cup without breaking, or to lift a heavy metal cup without dropping it. The inability to perform these types of tasks adds to user frustration and limits their ability to perform everyday tasks.

2.6 Visual Object Recognition

Visual object recognition is recognizing an object of interest within a digital image or a video. It can be achieved using cameras and software. Object recognition is used in several industries all around the world. However, in prosthetics, it is not a widely-used concept.

3D Imagery

Pictures taken with an average camera or smartphone produce two-dimensional images, meaning they lack depth information. In order to autonomously pick up objects, the prosthetic hand must be able to produce three-dimensional images of the object it is trying to identify. 3D images can be obtained with certain types of cameras, LIDAR sensors, or a combination of sensors. Any device or sensor that produces a 2D image and can sense depth, can create a three-dimensional picture of objects.

Point Clouds

An object can be broken down into a series of points, each with an x, y, and z location. These points create a point cloud within a given coordinate system, see Figure 25. Some cameras can create these point clouds with lasers or stereo imaging.

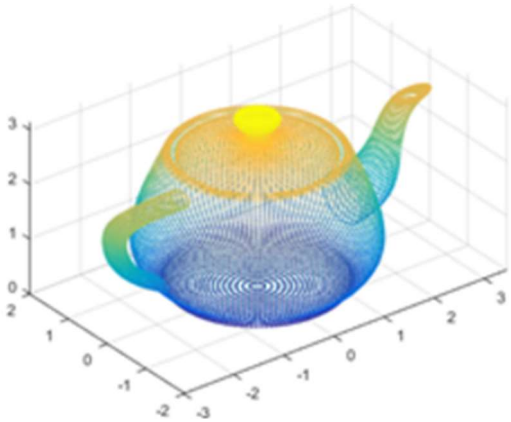

Figure 25: 3D Point Cloud of Tea Pot (3-D Point Cloud Processing, n.d.)

Point clouds can be used as a 3D imagery tool to view depth of objects in an environment, which can be used for a number of robotic applications including robot navigation and depth estimation (3-D Point Cloud Processing, n.d.). The clouds can be individual or compounded with multiple scans to create a single complex image, like the one in Figure 26. Individual points can be filtered out to create smoother images and reduce mistakes created by noise.

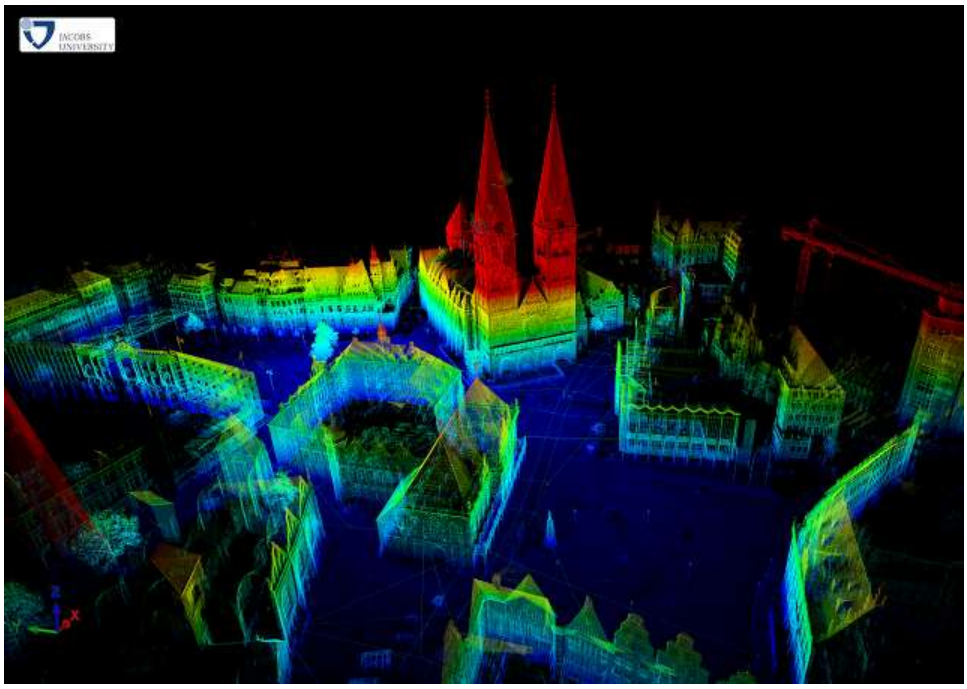

Figure 26: 3D Point Cloud of Bremin City Center (Borrmann, D., & Elseberg, J., n.d.)

Point clouds offer a means for this prosthetic to view images in 3D. The point cloud can be used to determine an object's depth or distance to the camera, while filtered data could provide the size and shape.

3. Project Strategy

The goal of this project is to create a smart transradial prosthetic device that integrates visual imagery with orientation, force, and angle feedback to autonomously grasp common items.

3.1 Initial Statement of Need

This project was done within the Soft Robotics Lab at WPI. Previous iterations of this project, see Section 2.4, were also conducted in this lab. Our team was asked to complete the full design, assembly, and successful testing of a hand, wrist, and forearm. As this project has been in progress since 2012, the statement of need given by Professor Onal was to fully fabricate and test a device.

Although no previous MQP was successful in completing this device, the past successes and failures were taken into consideration when addressing our project goals. The only features maintained from past versions of the hand were the fingers and thumb, as they both proved successful at completing the necessary range of motion for a variety of grasps. All other components of the device were developed by this year's iteration of the MQP.

3.2 Design Requirements: Technical

3.2.1 Objectives

The project was broken down into six main objectives:

1. Design and prototype a functioning robotic prosthetic hand.
2. Successfully complete the following tests:
    a. Grasp a mug and move without spilling the liquid.
    b. Grasp soft and fragile objects without causing damage.
3. Create a system that can recognize objects in the environment.
4. Integrate the device with object classification software.
5. Autonomously detect and grasp an object in the environment.
6. Provide sensing feedback as the hand moves throughout its environment.

The device is considered fully functional once these required objectives have been completed. Any secondary objectives such as improving comfort, adding features, and further improving the effectiveness of the software will be considered only if time allows.

3.2.2 Design Constraints and Specifications

User Interface

- Battery must be accessible and hot-swappable with one hand and screwdriver.
- Must be able to remove battery for recharging.
- Pins must be accessible for maintenance and testing.

Human Features

- Device must resemble an adult human hand and forearm.
- Hand, wrist, forearm, and self-contained power must weigh less than 1,750g.
- Must have a carrying capacity of 1 kg offset by 10 cm to the palm's center of mass.

Mechanical

- Palm must be able to fit all motors, potentiometers, sensors, camera, and an IMU.
- Forearm must be able to fit all motor drivers, batteries, and a microcontroller.

- Thumb, index, middle, and ring finger must be able to move independently and simultaneously.

Electrical

- Less than 20 wires connecting the forearm to the palm.
- Wires must not run through or underneath gears.
- All potentiometers must be secure within each knuckle.
- Each independently moving finger must have at least one force sensor to feel its environment.

Control

- Device must sense the orientation of the palm within 5 degrees of accuracy.
- Each finger must be able to open or close fully within 2.5 seconds.
- Must be able to complete a full power grasp.

Cost

- Total cost of device must be lower than $1,500.

Safety

- Arm must be made out a material that is safe for humans.
- Device must not put user in any immediate risk during use due to exposed electrical connects or potential pinch points.
- All movement must stop if control signal is lost.
- All motors must have software limits to prevent self-destruction of hand.

3.3 Design Requirements: Standards

Since this device was developed for research and non-invasive purposes, and does not use any biological material, there were only a few standards considered in its development. The largest consideration was in material choice, as the prosthetic would need to be safe for extended periods of human exposure and safe for contact with food. Since this device was to be 3D printed, ABS was selected as the material. ABS is certified for prolonged human exposure and is compliant with FDA regulation for food exposure according to FDA Title 21 (21CFR177.1020). The material selected for a silicone cover was also food-grade and made with FDA-listed materials for food safety.

In the future, if this device is to be used or tested on amputees, there are a few ISO standards that need to be considered. Namely ISO 8548-3:1993 which standardizes the method of describing and recording information for upper limb amputations. If any portion of the device is to come in contact with the amputee's skin and not a socket, ISO 10993-10:2010 should also be taken into consideration so that the device meets all tests for potential skin irritation.

3.4 Revised Statement of Need

After reviewing current prosthetics on the market and the work completed by the past MQP's, the team assessed the functionality versus the price of current prosthetics to best revise the statement of need. Based upon Table 3, each device was given rankings based on the number of grips, maximum grip force, device weight, functional wrist, and method of powering the device. Rankings were classified as follows:

- Grip: score based upon number of possible grips (for hooks number of grips was set as 1).
- Force: ranked based on maximum force during a power grip where 1 was the lowest and 6 is the highest.
- Weight: ranked where the lowest weight was a 6 and the highest was a 1.

- Wrist: 1 if there is a wrist and 0 if there is none.
- Power: 2 if myoelectric and 1 if body powered.
- Functionality: sum of all classifiers where the highest score meant highest degree of functionality.

The rankings and total functionality for each device is as follows in Table 5.

Table 5: Functionality Matrix for Current Market

Device	Grip	Force	Weight	Wrist	Power	Functionality	Cost ($)
Axon Hook	1	5	5	1	2	14	15,000
Grip 5 Prehensor	1	1	6	0	1	9	1,200
Michelangelo	7	3	3	1	2	16	75,000
I-limb ultra	14	4	2	1	2	23	17,000
BeBionic	14	6	1	1	2	24	11,000
Ada Hand	5	2	4	0	2	13	700

These findings were plotted as functionality versus cost to assess the current state of the prosthetic market. As shown by Figure 27, there are both low-functioning, low-cost and high-functioning, high-cost hands available on the market. However, there are no high-functioning, low-cost hands. To get any level of high-functionality, which based upon the mean of all prosthetics sampled is a rating of 16.5 or higher, there is a minimum price of $11,000.

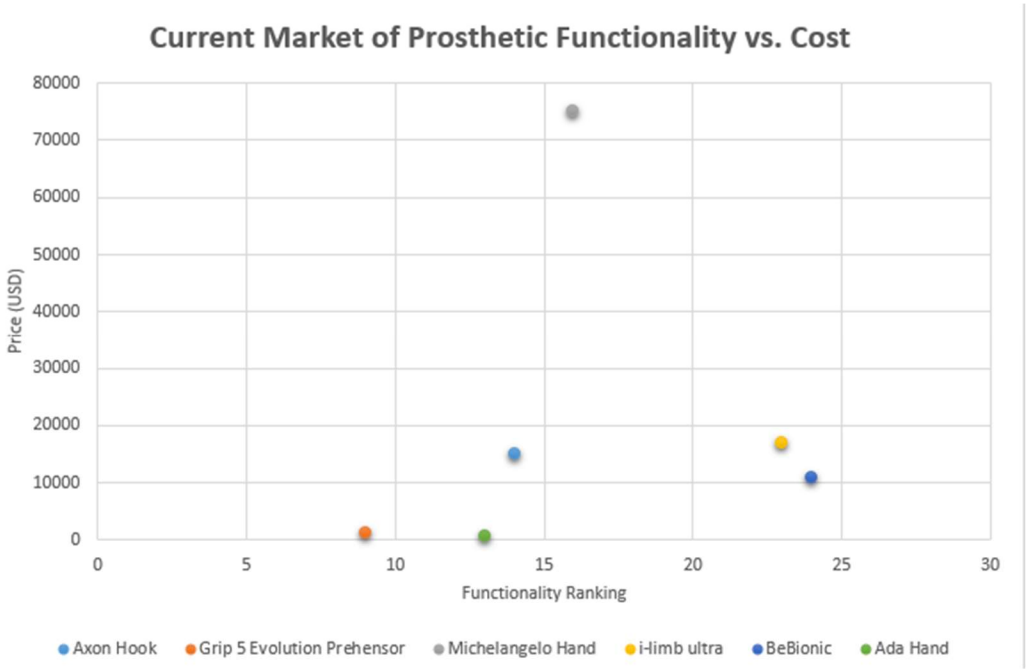

Figure 27: Current Market of Prosthetic Functionality vs. Cost

Taking this gap in the current prosthetic market into consideration, the team decided to adjust the statement of need to better facilitate the needs of both the project advisor and the current market. Thus, the statement was adjusted to completing the full design, assembly, and testing of a prosthetic hand, wrist, and forearm that is both high-functioning and low-cost.

4. Initial Prototype

The design portion of the project was divided into two prototypes. The initial prototype was designed based on the background research, past projects, and specifications discussed previously. This prototype was simulated and fabricated to find design flaws. The second and final prototype was created by redesigning the initial prototype to address all problems faced during assembly and testing. Since these two prototypes were designed and tested as individual entities, the design process has been outlined for each separately.

4.1 Mechanical Design

When designing the initial prototype, the entire assembly was broken down into three smaller subsystems: the hand, wrist and forearm. Each of these subsystems is discussed in greater detail in this section.

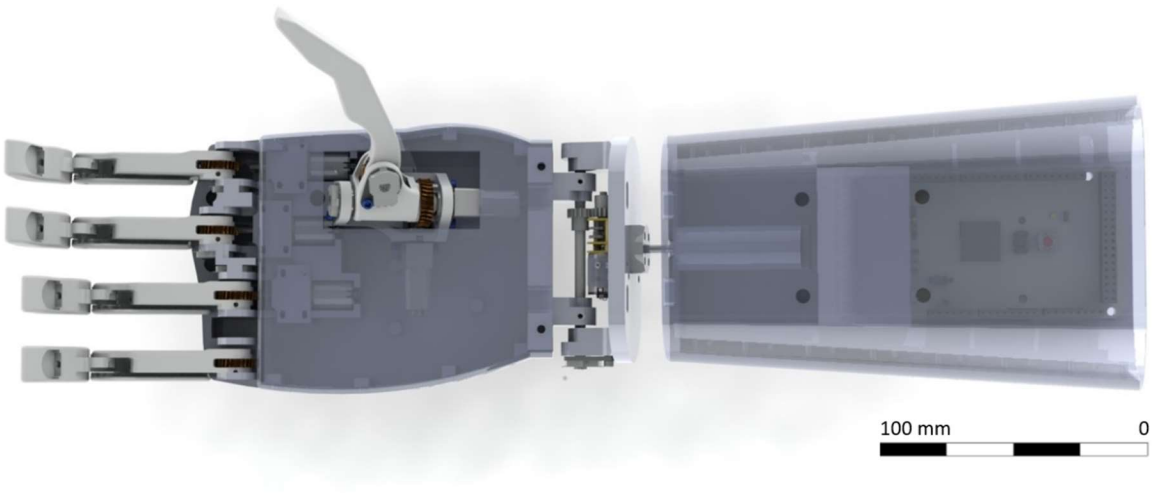

Figure 28: Full Assembly of all Mechanical Subsystems for Initial Prototype

4.1.1 Finger

As previously stated, the team decided to keep the finger and thumb designs developed by the past years MQPs. This design uses a worm and spur gear to power a four-bar linkage and allows a finger curl of up to 90 degrees. Since this worm gear design does result in a bulkier knuckle area the team considered using string tendons or a belt system to power the finger, however the worm gear remained the best option after careful consideration due to the increase chance of slack, increased difficulty in assembly, and the lower maximum possible force that tendons and belts introduced to the system.

Initially, when looking at the Frankenhand finger design there were two issues: loose potentiometers and small wire holes (Merlin, M. & Sullivan, K., 2016). As previously mentioned, the potentiometer was not secured to the knuckle, but glued to its side. This caused the potentiometer to potentially move or fall off while the hand was being operated. To fix this mechanical issue, the knuckle design was modified. Instead of placing the potentiometer outside of the knuckle, the knuckle was widened so the potentiometer could be placed inside. One wall of the knuckle was slotted so the device could slide into the knuckle. The slot had three walls to eliminate rotational movement, while the finger joint pressed the potentiometer into the knuckle to restrict forward and backward movement.

Another minor change to the finger design was the wire hole. In the Frankenhand design, these holes were very small, meaning that the wires connecting the force sensors to the hands also had to be small (30-gauge) to fit through the hole (Merlin, M. & Sullivan, K., 2016). This led to further problems, as thin wires break easier and have trouble sending power to the sensor and data back to the palm. To address this issue, the holes were widened to accommodate two 22-gauge wires.

Once these two design changes were made, a single finger was sent to be 3D printed with an onyx filament. Onyx filament is nylon based with micro-carbon fibers inside for reinforcement. This material is much stronger than the past iterations' materials. The previous prototypes of the hand broke very easily, leading to problems testing with the IRIS Hand and faults with Frankenhand (Casley, S. et al., 2014 and Merlin, M. & Sullivan, K., 2016). Since there are a number of small, fragile parts within the finger, the team felt this material would help to strengthen the overall hand. Onyx would make the hand more durable for everyday wear-and-tear and allow the hand to bear more weight than past versions. This finger design can be seen in Figure 29 below.

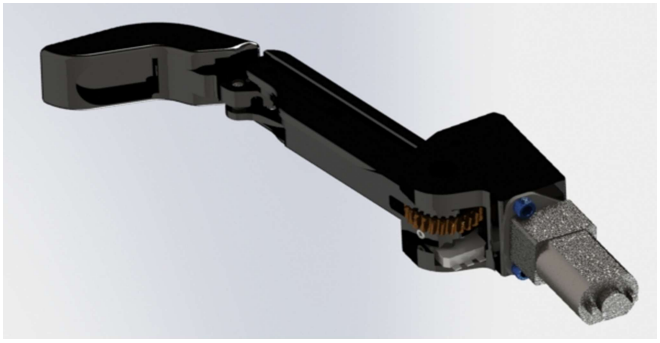

Figure 29: Edited Finger Assembly

The onyx material proved to be quite strong and flexible, however the quality of print was insufficient for testing. This led to another revision of the design. While the design remained largely the same as before, two parts of the top finger joint were modified. The wire hole for the force sensor removed too much of the support material for the joint connecting the top and bottom links. This caused the metal pin to shift at an angle, restricting the movement and cracking the thin material at the end of the link. This was fixed by removing the hole entirely, routing the wires down the side of the finger instead of inside.

The second problem with the new design was the knuckle. The slots for the potentiometer made the knuckle wall too thin, causing it to break if any substantial pressure was applied. In order to maintain an appropriate thickness, while still securing the potentiometer in place, the knuckle portion of the finger assembly was removed entirely and incorporated into the palm design.

4.1.2 Palm

To reduce the space needed for the knuckles, the palm was redesigned to fuse the two components together. The mechanisms were maintained; however, the gears and motors were attached to the top plate of the palm instead of a separate knuckle. The space between the knuckles was used to direct wires away from exposed motors and gears. Since none of the grips need all the fingers to move independently of one another, and to capitalize on usable space, the ring and little fingers were coupled together. This means that the two fingers share a shaft and are powered by a single motor, located below the ring finger.

This modification reduces the palm's weight, size, and complexity, while creating more space for electrical components.

This palm also allowed for a better method for securing the potentiometers. To eliminate the potential movement, and thereby inaccuracy of the potentiometers, a casing was added on one side of the knuckle. This case was an open box slightly lower than the rest of the knuckle. This allowed the potentiometer to slide downward into position where it could be secured with the D-Shaft. The slot was tight fit to eliminate forward and backward movement and had a top and bottom to restrict rotation.

There were several other problems with the previous versions of the palm, including size and shape. The overall shape of the palm was modified to reduce the rectangularity and to more closely resemble a human hand. Curves were added to the sides of the palm, knuckle bumps were added behind each finger, and a slope was added to the top plate. These additions created a more natural look for the prosthetic hand.

Despite the strength of the onyx material, the time delay and poor quality made the filament impractical for the first prototype. The Frankenhand palm was 3D printed using ABS filament, which proved durable enough to withstand substantial applied force, even at the thinnest of areas (Merlin, M. & Sullivan, K., 2016). While the material was strong, the thickness of the walls ranged from 2 to 8 mm. To create more uniformity in the piece and increase usable space, the wall thicknesses were all set to 2.5 mm. This new sizing made connecting the top and bottom plates more difficult, so supports were added behind each screw hole.

The new design also created modularity between the palm, wrist, and forearm. The end of the palm was a hollow socket with four screw holes. The top piece of the wrist fit inside this socket and could be secured with screws on both sides. This allows for the modification of either section without having to reprint the entire device. This modularity could also be used to personalize each prosthetic in manufacturing. The CAD model of the redesigned palm is shown in Figure 30 below.

Figure 30: Initial Prototype Modular Palm CAD Model

4.1.3 Wrist

No previous version of this project had a fully operational wrist, so none of the past wrist designs were considered. Instead, the team analyzed two potential joints: ball-and-socket and universal. Both of these options would create a more natural wrist movement than belts or hinges. The first joint considered was the ball-and-socket. This joint allows for three degrees of freedom and smooth, continuous motion. The design requires three motors, one for each degree of freedom, and linkages between the wrist and forearm. While the wrist could rotate very well, the design involved complex motion, in-depth motion analysis, and added excessive weight to the small wrist.

The next joint considered was the universal joint. This joint, illustrated in Figure 31(a), consists of two coupled shafts that allow for rotation about two axes. Two motors actuate the rotation about the x- and z-axis, which will allow for hand flexion/extension and circumduction respectively, these axes are summarized in Figure 31(b). While the movement consists of one less degree of freedom than the ball-and-socket, the simplicity of the design made it more desirable for the project objectives.

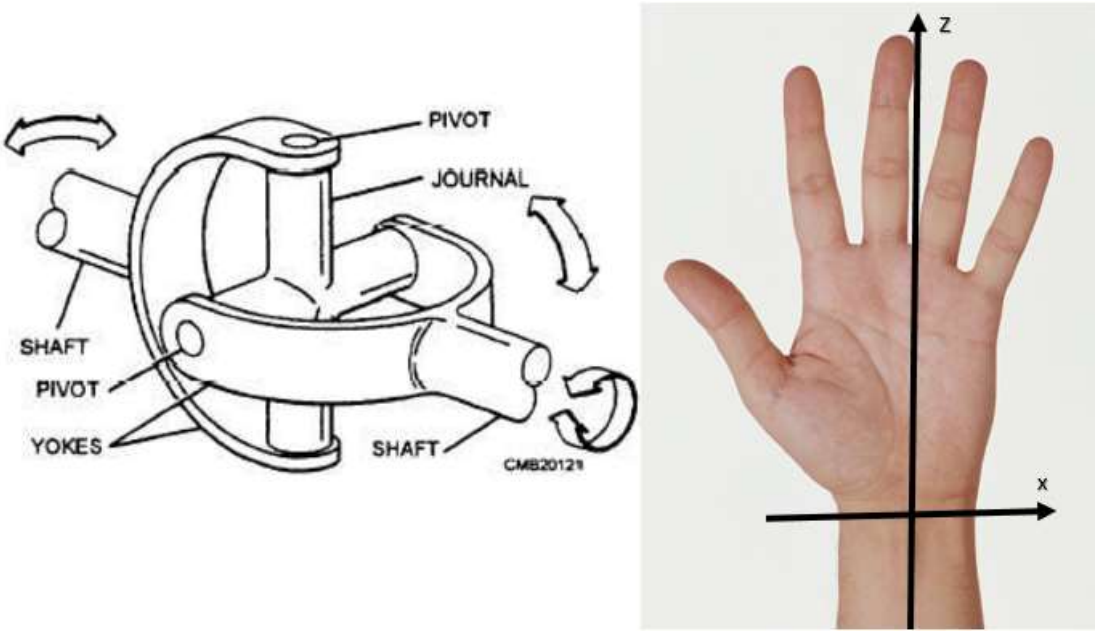

Figure 31: (a) Illustration of a Universal Joint (Cross and Roller Universal Joint, n.d.) and (b) corresponding rotations in the wrist.

The wrist was designed to be entirely modular from the palm. The joint is divided into two parts: a socket-like connection to the palm and a connection to link with a motor shaft in the forearm. Both sides of the wrist are connected by the x-axis, as shown in Figure 32 below. This CAD model also shows that the rotational shafts are not connected as they are in a typical universal joint. Instead, the shafts were offset from each other to allow for a simpler design and make better use of the available space.

Movement along the x-axis is driven by a Pololu motor and two plastic spur gears. Bearings on either end of the shaft attach it to the bottom portion of the wrist while a tight fit attaches the shaft to the upper portion of the wrist to control movement. The motor is secured to the wrist by set screws threaded through L-brackets supports on either side. X-axis movement is driven by a motor in the center of the forearm. A universal mounting hub at the bottom of the wrist is used to couple the motor shaft to the wrist, as shown in Figure 33.

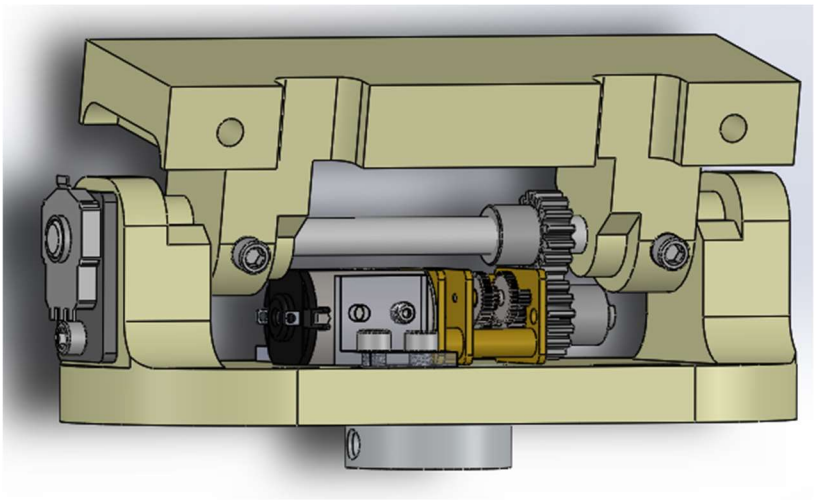

Figure 32: Side view of the wrist: upper link connects to the palm while the bottom link connects to the z-axis motor shaft.

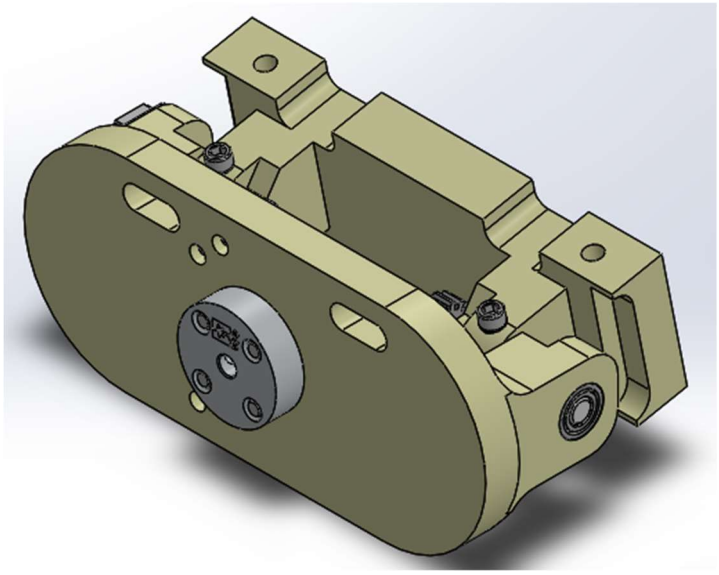

Figure 33: Bottom view of the wrist, showing universal mounting hub for forearm connection.

4.1.4 Forearm

To maintain a modular design, the forearm was created as a separate component of the overall design. The wrist and forearm are connected by motor shaft that extends out of the forearm into a universal mounting hub. This motor provides the z-axis rotation. The distal end of the forearm is the same size as the bottom wrist, but gets gradually larger as it extends, ultimately ending in a 1 cm offset on the proximal end of the forearm. This creates a more realistic, human-like tapered appearance than a circular or rectangular cross section. The length of the forearm was set at 16 cm, as this is about ¾ of the length of the average male forearm. Although a point of connection with the residual limb has not been designed within the scope of this project, this length may provide enough room to do so.

Space within the forearm is meant to house most of the electrical components necessary for powering the prosthetic. As shown in Figure 34 below, the forearm houses the microcontroller, which is mounted on the forearm with screws, in addition to the battery pack, which will be attached using Velcro strips.

Velcro was chosen since it is affordable and allows for easy removal of the battery for charging. Seven slots were created along the sides of the top plate. These slots allow for the placement of protoboards during the electrical assembly. Six screw holes were added to each side of the forearm to attach the top and bottom plates. The same screws and inserts were used for both the palm and forearm for uniformity.

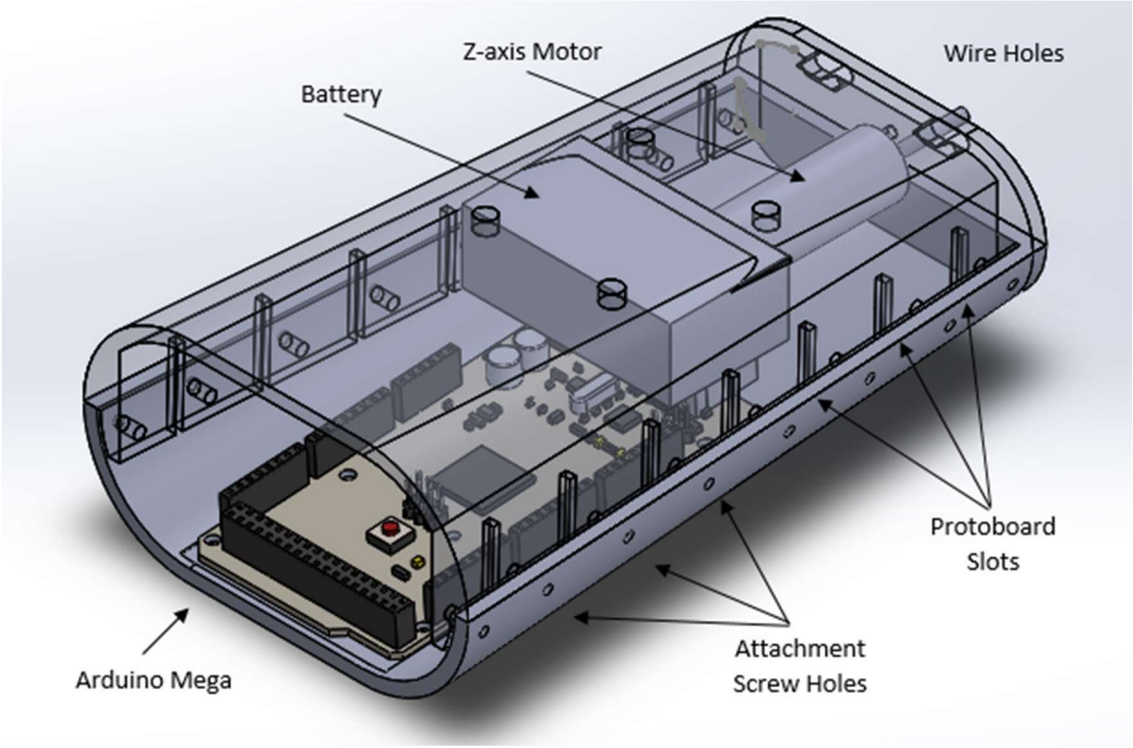

Figure 34: Forearm model showing sufficient space requirements for large electrical components as well as mechanical features.

4.2 System Architecture

The system architecture can be found in Figure 35. The figure illustrates the inputs and outputs of each electrical component and its location within the system. The Arduino Mega 2560 microcontroller is used to gather all the input signals.

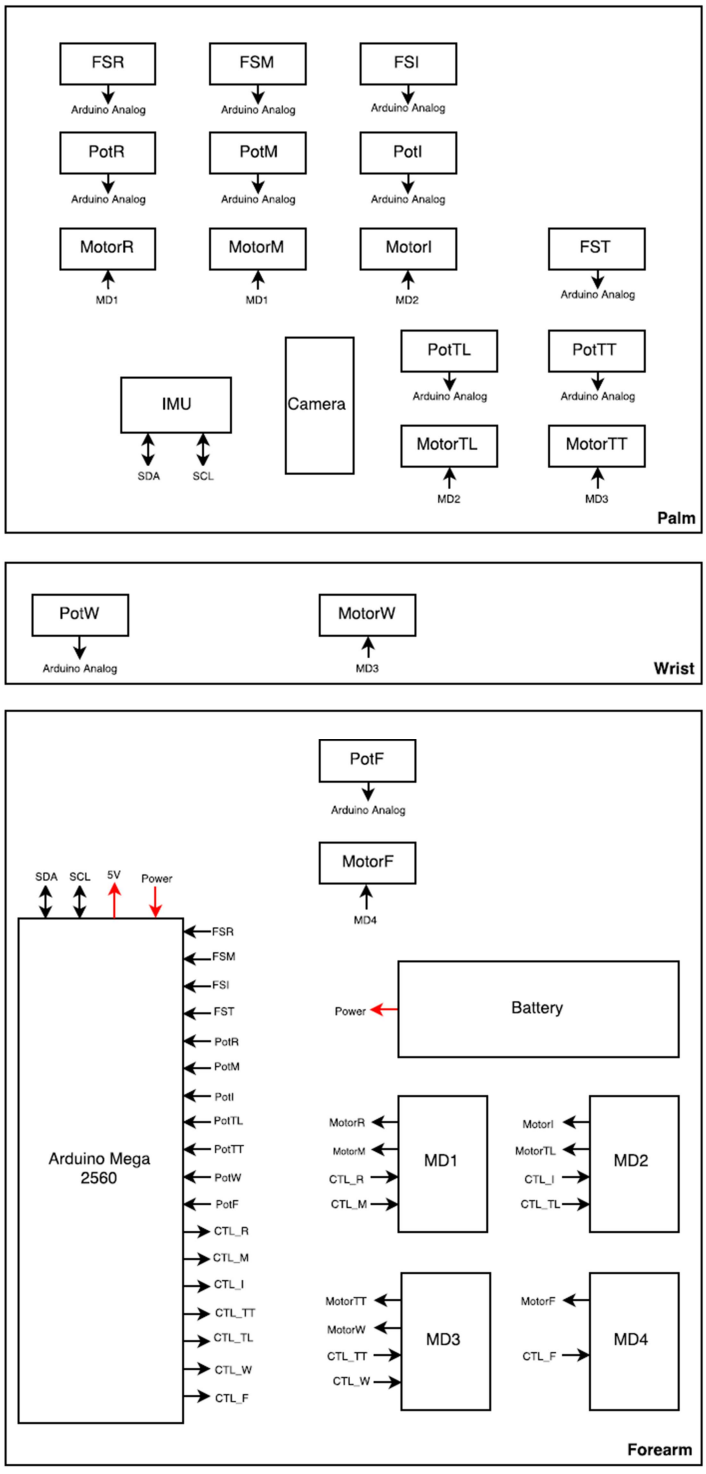

Key	
R	Ring Finger
M	Middle Finger
I	Index Finger
T	Thumb
TT	Thumb Top
TL	Thumb Left
FS	Force Sensor
Pot	Potentiometer
MD	Motor Driver
IMU	Inertial Measurement Unit

Figure 35: System Architecture Diagram

4.3 Electrical Design

4.3.1 Electrical Subsystem

The electrical system for the initial prototype is illustrated in Figure 36. This diagram is a simplified version of the architecture for the motors, microcontroller, and sensors.

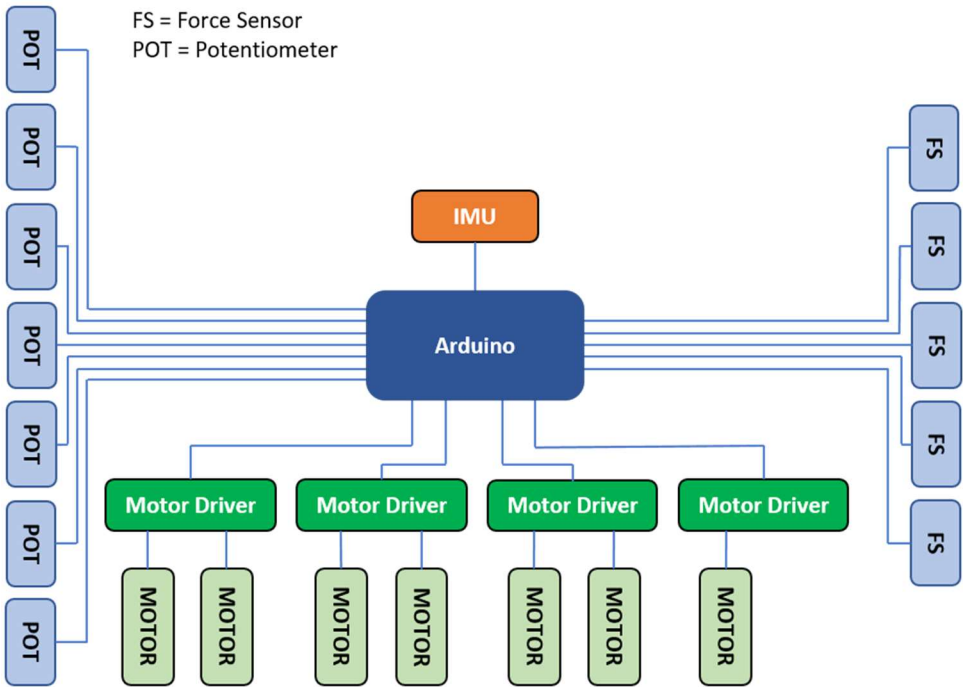

Figure 36: Electrical Subsystem for the Initial Prototype

4.3.2 Finger

For the initial prototype, each finger fits one force sensitive resistor in the top joint. Force sensors give the hand the ability to precisely hold items without crushing or dropping them. These force sensors are connected directly to the digital I/O pins on the forearm's microcontroller. These pins provide 20 kΩ pull-up resistors, which eliminate the need to attach separate resistors to each force sensor wire.

4.3.3 Palm

The palm houses all of the finger motors and potentiometers. There are five motors in total: three for the fingers and two for the thumb. They are high-power 6V Pololu 1000:1 Micro Metal Gearmotors with a stall current of 1600 mA. Each motor has its own potentiometer attached for angle feedback during actuation. An Inertial Measurement Unit (IMU) was placed in the center of the top plate of the palm. This component uses gyroscopes and accelerometers to measure the change in acceleration and movements of roll, pitch, and yaw. As the hand moves about its environment, the IMU is used to determine the palms orientation with respect to the forearm.

4.3.4 Wrist

There is one motor located within the wrist to control the x-axis rotation. Due to the compact size and high torque needed for this joint, 1000:1 Micro Metal Gearmotor was used. A rotary potentiometer was placed on the x-axis shaft to send angle feedback to the system.

4.3.5 Forearm

The forearm houses the microcontroller, motor drivers, battery and one of the motors for the wrist actuation. A motor was added to the system to control the z-axis wrist rotation. There are seven slots in the top cover of the forearm to hold protoboard sheets. Each protoboard sheet is long enough to hold two motor drivers. Since only four motor drivers are needed for the device, the extra slots make the addition of electrical components much easier, as well as making maintenance simpler. To fix a broken motor driver, the rectangular protoboard can be pulled out and replaced with minimal soldering. These boards also help organize the wiring within the forearm.

4.3.6 Actuation

The first part of the electrical design is actuation. The microcontroller sends three signals (2 bits: direction and PWM) to the motor drivers to control the movement. The Arduino Due of the past iterations of this project was discontinued by the manufacturer. Since future manufacturing of the device would be affected by the discontinuation, the microcontroller was changed. Both the Arduino Mega 2560 and the Raspberry Pi 3 were considered. While the Raspberry Pi 3 has WiFi capability and a smaller size, the ease of programming and the number of pins on the Mega made it the better choice to control the device. The Mega also has more PWM outputs, analog inputs, and a more convenient operating voltage, 5V as opposed to 3.3V, than the Due.

The previous finger design, as used by Paul Ventimiglia and Frankenhand, was kept. This design featured a 1000:1 Pololu micro metal gearmotor to control individual fingers. Each motor requires a motor driver, with two motors per motor driver, so four were added to the system. Located in the forearm, the DC motor driver breakout boards amplify the current passed to each motor. These drivers control the three finger motors (one for ring and little finger combined and one each for index and middle finger), two thumb motors, and two wrist motors.

The two types of rotation in the wrist are also controlled by DC motors. The rotation about the x-axis is actuated with the same 1000:1 Pololu micro metal gearmotor. The wrist and forearm are connected to the forearm by a single shaft, allowing for independent rotation about the z-axis with a brush DC motor.

A single battery provides power to the microcontroller board and motor drivers. While several batteries were considered, a 11.1V, 730 mAh Thunder Power RC lithium polymer battery was chosen over NiMH, NiCd, and lithium ion, since it is more compact.

4.3.7 Sensing

For sensing, the hand has an IMU, five force sensors, and seven potentiometers. Located in the palm, the IMU is used to sense the orientation of the palm at all times. This helps the system to maintain the proper orientation while moving objects, therefore reducing the possibility of spilling an object's contents.

To measure the angle of the fingers and wrist during movement, each motor has a potentiometer attached to the shaft. The process in selecting in between encoders attached to the motors and potentiometer attached to shafts, team went with potentiometers because the palm does not have enough space behind the motors for the encoders. Encoders might be easier to use, however for sizing concerns, potentiometers were better fits for this project. Since the ring finger is coupled with the little finger, the two share a potentiometer. The thumb and the wrist each have two sensors, one for each axis of rotation.

There are five force sensors in the hand, one for each finger and the thumb. Located in the tip of the finger, these sensors measure the amount of force on each finger as it grasps and lifts an object. The sensor is rated at 1.96 N - 19.6 N of force and has a moisture sensitivity level of 1, meaning it will work in moisture for an unlimited amount of time.

To package all the analog signals, force sensors, and potentiometers, an analog to digital multiplexer (MUX) was added to the hand. This device sends packaged data through the I^2C communication protocol. The addition of a MUX to the system also greatly reduces the number of wires connecting the palm to the forearm.

Since there are a large number of wires and electrical components needed within the palm, a custom-cut protoboard was added on the top plate. The MUX and IMU were soldered to the protoboard, rather than secured to the palm itself. The addition of this board makes modifying the electrical components much easier, as the whole board can be removed at one time. The board also helps organize the wires inside of the palm. Instead of connecting the motor and force sensor wires directly to the MUX, which could cause them to run underneath or through gears, the wires can be directed to an empty portion of the palm. These wires will be soldered to the protoboard with a jumper wire connected to the MUX. This protoboard is shown in Figure 37 below.

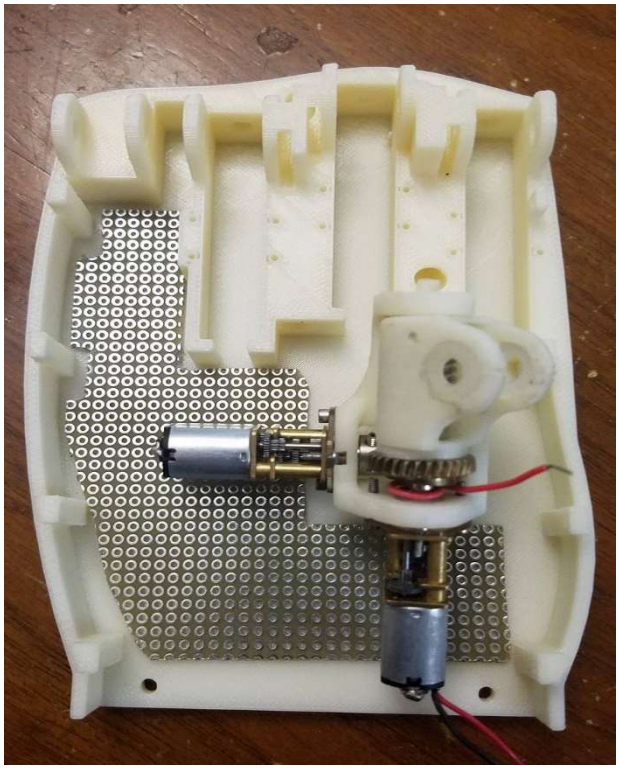

Figure 37: Protoboard in the Palm Prototype

4.4 Initial Prototype Assembly

The team decided that building two prototypes would be necessary for the success of this project given the intensive redesign of the previous years' designs. Thus, the purpose of building the initial prototype was to find any design problems, so that alterations could be made before the final device. This would

lead to a more robust and successful final prototype. During initial prototype assembly, any issues with the overall mechanical and electrical structure was well documented so that changes could be made in the final prototype.

4.4.1 Palm

The palm and fingers were 3D printed with high density ABS filament on a Dimension printer. The first component assembled was the palm. The motors fit perfectly in their slots, without the need for extra spacers at the end. The screw holes for the motor brackets, however, were too small. Each hole was drilled out to the correct size and hand-threaded with a screw, as there was no tap small enough to fit. Once the holes were widened, the brackets were attached and the motor was firmly held in place on four sides.

The knuckles were modified next. Access to the middle knuckle was tighter than anticipated, so the potentiometer slot between the index and middle fingers was sanded down with a Dremel. While this allowed better access to the shaft hole, the Dremel also removed some of the index knuckle. This cut had no effect on the finger support, but it removed the section needed for the linkage pin hole. This hole was drilled into the remaining three finger knuckles.

The slots for the potentiometers were created with a 1 mm tolerance, however the fit was tight when printed. To reduce the amount of force needed to push the potentiometer in place, which also put strain on the wire connections, the plastic supports on the potentiometer were sanded off. This allowed the potentiometers to slide in with less effort, making them easier to attach to the metal shaft.

McMaster heat-set inserts were placed in all of the attachment holes. A soldering iron melted the surrounding plastic around the insert, securing it in place. These inserts are threaded to make screwing the top and bottom covers easier. The plastic supports around the insert were not wide enough, so they cracked or bent while the inserts were being placed. This made attaching the cover more difficult, as only four of the ten screws were usable.

There were several problems with the top cover. The top side of the cover hit the wire connections for the finger potentiometers, making it impossible to screw the two plates together. The set screws on the index and ring fingers also collided with the side of the case as they rotated through their last 10 degrees of movement. To fix these issues, the top side of the cover was sanded off with a Dremel. The square hole surrounding the thumb was also extended to provide clearance for the potentiometer connected to the top rolling link.

4.4.2 Fingers

Once the palm was assembled, the top and bottom links of the fingers were secured with a pin. The removal of the force sensor wire holes gave the new pin holes enough support to move correctly without cracking. The linkages were connected to the joint with the same pin and secured in place by the finger wall. The final joint was coated with adhesive for extra durability. The gear at the bottom of the finger has a slight rotation when connected to the motor, as there was only one hole to secure it to the finger. This was temporarily fixed with liquid superglue. Once the glue was dry, the assembly was placed in the correct knuckle and secured with the shaft. The assembly of the fingers and palm can be seen in Figure 38.

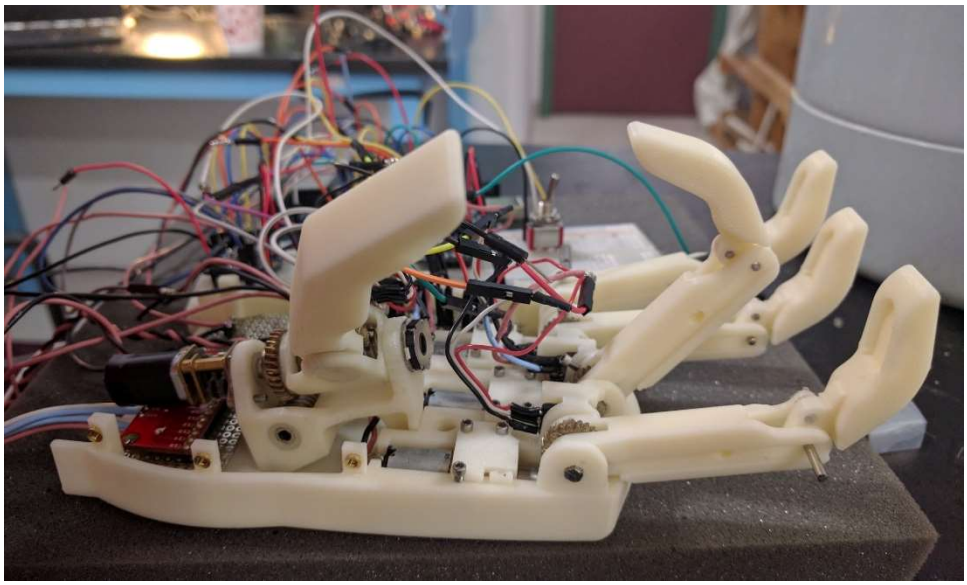

Figure 38: Assembly of Fingers and Palm without Force Sensors

There was excess slack in the fingers due to the set-screws in the shaft. The shaft was cut to fit the individual fingers with the end of each shaft sanded into a D-Shaft to fit the potentiometer. Since the remainder of the shaft was circular, the set-screws did not have much hold and caused a delay in the finger movement. This slack was temporarily fixed with adhesive, but a more permanent solution was needed for the final prototype, as it caused positioning errors while testing the finger grasps.

The force sensor hole was designed for a thicker device, so the sensor would not contact the object during grasping. To prop the force sensor up, a metal hex nut was placed between the finger and the sensor. Since the sensor pushed up against a hard, flat surface, the reading was more sensitive. This helped with testing object grasping.

Since there was no slot on the thumb, the force sensor was glued to the surface. The remaining thumb was reused from the Frankenhand prototype. The assembly was secured to the palm with three hex screws.

4.4.3 Wrist

The wrist was designed and manufactured in two parts: bottom link and top link. The first piece assembled was the coupler that attached the bottom of the wrist to the forearm motor shaft. This component was screwed into the bottom joint with four screws. Then, using a U-shaped 3D printed bracket, the x-axis motor was attached to the top plane of the bottom link.

The bearings for the top link were placed, however the holes were tighter than expected and there was not enough support material around the hole. This lead the plastic to crack and break off over repeated testing. This was temporarily fixed with adhesive and tape.

When the circular shaft was placed through the plastic gear, there was no set screw. To ensure the shaft and gear rotated together, the two were glued together. Another plastic gear was attached to the motor shaft with a set screw and the two links were joined together with the shaft. The alignment of the components proved difficult, as any misalignment caused the gears to unmesh or skip. There were

multiple attempts to fix the alignment and reduce the slack in the joint. The final solution was to secure the motor on both sides with metal L-brackets. These supports were screwed and glued on either side of the motor to eliminate side-to-side movement while the wrist was moving, as this would cause the gears to unmesh entirely. Once the motor was fixed in place, the end of the shaft was modified to be a D-Shaft and a potentiometer was attached. The assembled wrist can be seen in Figure 39.

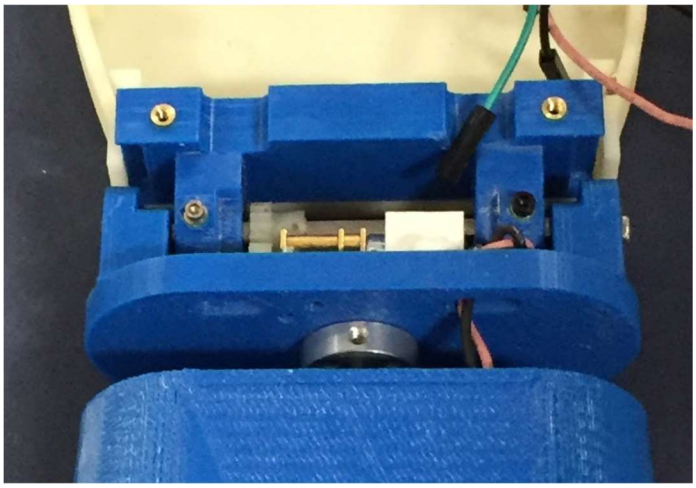

Figure 39: Assembled Wrist

When the wrist was connected the palm, the top surface collided with one of the thumb motors. If the wrist was fully attached, this motor would not work correctly, as the connection wires were affected by the pressure. For testing, the wrist was sanded down and screwed in only one side.

4.4.4 Forearm

The forearm was designed after the palm, so it needed fewer modifications during assembly. The supports for the screws were widened and thickened to reduce the risk of breakage. This design worked far better than the palm and there were no problems placing the heat-set inserts.

Once the motor was screwed into the bottom plate, a potentiometer was attached on the outside cover. Since there was no attachment method for this device, the potentiometer was secured with tape. The wire holes on the cover were also widened to allow the wires to move more easily with the wrist.

The Arduino was secured to the bottom plate with four screws. Originally the design had the USB port facing the motor, but this became too difficult to plug in while testing, so the Arduino was rotated 180 degrees to face the larger, proximal end of the forearm. Since the holes were not in the same spot on both sides of the microcontroller, only two lined up when the device was rotated. The two screws securely held the device, so no additional holes were drilled out.

4.4.5 Electrical System

As mentioned previously, a protoboard was used in the palm for the early stages of the initial prototype. The ADC MUX was incorporated to decrease the number of wires travelling through the wrist, however the component caused a delay in the software while it switched between channels. Furthermore, the number of wires leaving the palm was below the desired specifications, making the MUX unnecessary. These factors, and the desire to make the palm as compact as possible, led the team to remove the MUX and protoboard from the prototype.

After these two components were removed, there were no further electrical modifications required for the palm. In the forearm, four motor drivers were soldered to protoboards (two per board), then all connections from the motors and sensors were put together and plugged into the Arduino Mega. All exposed wires were covered with heat-shrink tubes to protect the system from shorting and the user from harm if they touch exposed connections. As seen in Figure 40, all electrical components were able to comfortably fit within the compact mechanical design.

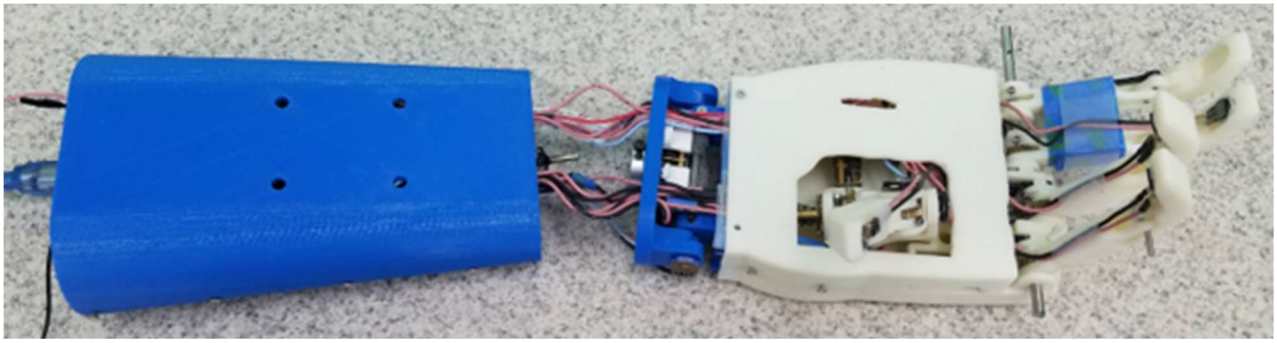

Figure 40: Initial Prototype Full Assembly

4.4.6 Software

The software for the prototype was aimed towards ease of testing. The project objectives were broken down into two main functions: self-balancing movement and grasping. The self-balancing mode required input from the IMU in the palm to compensate for the rotation in the hand, wrist, and forearm. The goal was to move a cup without spilling the contents. To accomplish this task, the IMU was used to monitor the angle in both the x and z-axis. For both axes, the IMU sent an angle from 0 to 360 degrees. This data was processed by the algorithm every time the code looped. During each loop, the algorithm compared the angle value to the last loop and mapped the value to a 0-1023(10 bit) range. This value was then fed to the P-Control as the target value.

The team learned that this approach was not the best way to convert IMU angles into a P-Control feedback, as the program set the current angle as the previous angle, causing the control loop to respond slower than the angle changes. This could be fixed in the second prototype by setting the initial IMU reading as the initial value and using the angles as P-Control targets.

The second task was grasping. For this, different control loops were set up to move the different finger motors. The target values were chosen through trial and error to grasp a cup and a cylinder. The control commands were all called in the same loop to ensure that the fingers move simultaneously. Since mechanical slack caused an unreliable grasping movement, the software needed further development and tuning for the second prototype.

4.5 Testing

For initial testing, the motors were driven for 2000 ms, then the direction was reversed for another 2000 ms. By timing the motors, the range of finger motion could be tested, despite limitations in potentiometer accuracy. Figure 40 below shows a side view of the hand with both the index finger and thumb curling into a pinch pose.

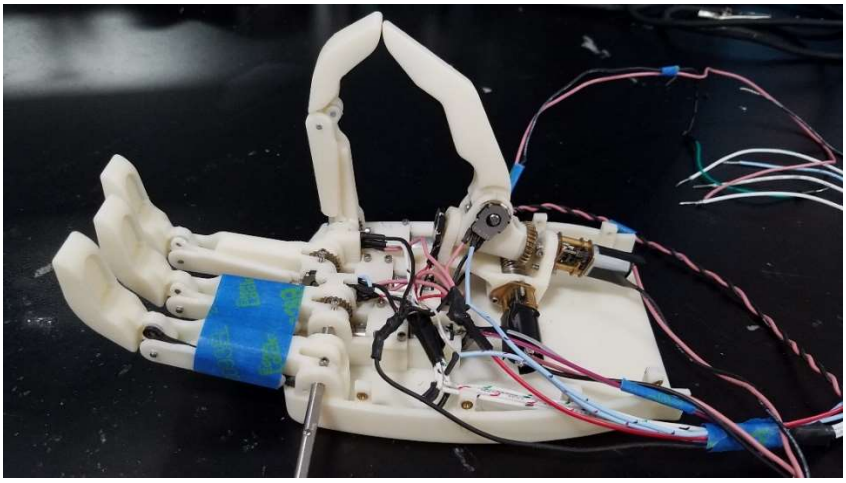

Figure 40: Side View of Hand Prototype

Testing for the device has been broken down into several steps. The first step was to use a solderless breadboard and Arduino Mega to test individual components. One force sensor was then connected to the MUX to see if communication with the Arduino on I^2C worked properly. While there was communication between the components, the speed of communication is limited by the pace of the MUX's switching between channels.

The MUX was then tested with inputs from potentiometers and the resistance-based force sensors, which were rated for 1.96 N to 19.6 N. For testing, the code was run in a loop with interrupts for faster results, as shown in Figure 41 below.

```
void loop() {
//Choose channel 15
  sendBinary15();
//Read the output signal
   readSignal();
 //Choose channel 13
  sendBinary13();
//Read the output signal
   readSignal();
 //Choose channel 0
  sendBinary0();
//Read the output signal
   readSignal();
      }
```

Figure 41: Testing of MUX

The next milestone was testing the motor drivers with analog inputs. Input values from the potentiometer were used to provide a reference position for the motor using PID controller. In order to do this, the potentiometer channel on the MUX was read and the value was converted into a direction and PWM

signal, which was then sent to the motor. During testing the signal was sent successfully as motor activation occurred.

The Arduino PID library was insufficient for this project, so a custom P-Control library[1] was written. This library made writing and modifying the control very easy.

As the assembly of the prototype progressed, the testing was modified. The IMU was attached to the palm cover and connected to the wrist. This allowed the team to test the self-balancing mode without the added weight of the palm. This separation also allowed a division of tasks, as the code could be written simultaneously with the assembly of parts.

To get the IMU feedback, the program used the Adafruit_BNO055 library (Townsend, K., n.d.). This is the library for the IMU that Adafruit provides, it contains communication protocols and functions that are useful for using the hardware. The algorithm for two degree of freedom balancing seemed to work, but slack in the mechanical components and weak motors caused the testing to fail. The motors did not have enough torque to hold the whole palm up. In addition to mechanical improvements, the next prototype code needs to feed the IMU data straight to the control loop to control the orientation of the palm.

Once the self-balancing mode was coded and the fingers had control, grasping was tested. To start, each finger was tested with the control loop to test movement, feedback, and range. All range values were recorded for future reference. Once the ranges were tracked, these values were added to the software. Each grasp had separate target potentiometer values defined and, depending on the test, were fed into the control loop. Every finger was able to move simultaneously without problem to the target values consistently. The device was able to grasp a ball, cylinder, and perform pinch grasp between the thumb and every finger. Figure 42 shows the pinch poses for every finger.

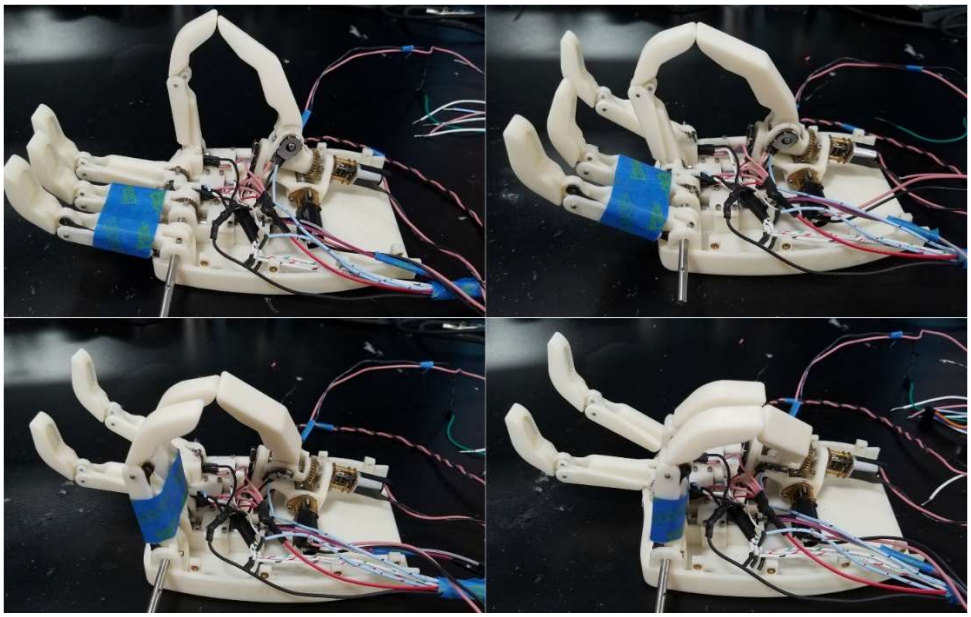

Figure 42: Finger Pinch Poses

[1] https://github.com/ybsipka/Dexter-Assistive-Intelligence-for-Transradial-Amputees

5. Final Prototype

5.1 Mechanical Design

Changes were made to the mechanical design to improve ease of assembly and better facilitate electrical components based upon design flaws found in the initial prototype. These changes led to an improved modularity and an overall more practical design, as seen in Figure 43. The final assembly of the prototype is shown in Figure 44 below.

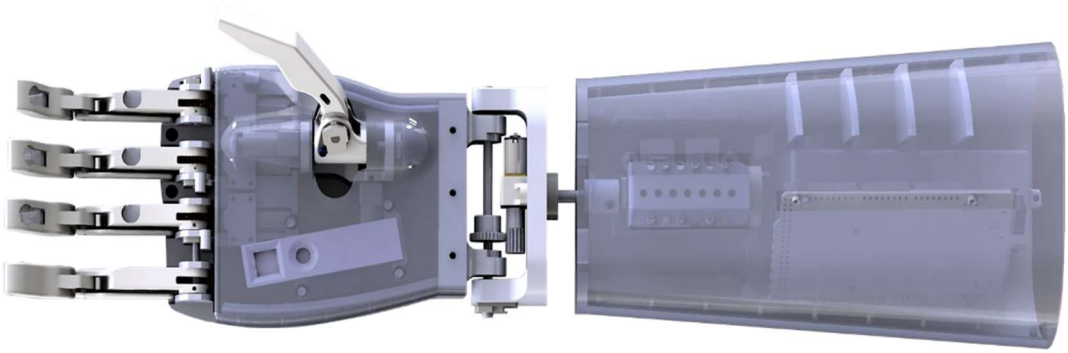

Figure 43: Final Prototype Full Assembly CAD Model

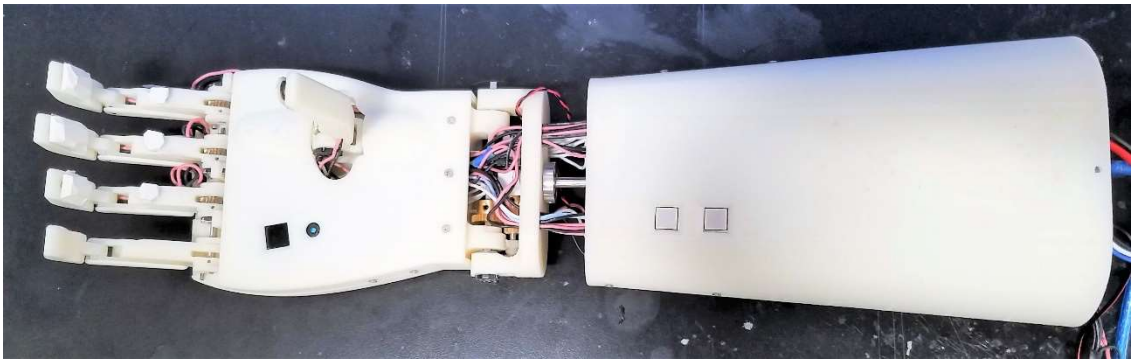

Figure 44: Final Prototype Full Assembled Device

5.1.1 Mechanical Subsystem Layouts

The final prototype can be broken down into three main subsystems: the hand, wrist, and forearm. Each subsystem contains different sensors and design elements that optimize space and functionality. Hand design was altered to look more anthropomorphic and serves as the housing mechanism for the finger motors, camera, IMU, and thumb. The placement of these components within the subsystem can be seen in Figure 45.

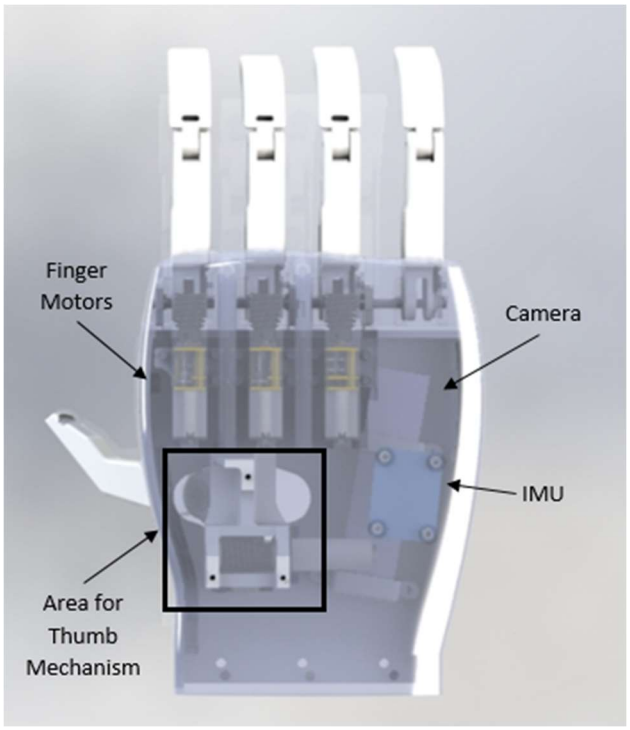

Figure 45: Key Components in Hand Subassembly

The forearm was the other subassembly to get a major redesign in system layout. Major additions to the forearm are shown in Figure 46 and Figure 47 below. A z-axis motor shaft extender and two touch sensitive buttons for control of the device were the two key elements added. Aside from that, battery and Arduino placement was modified to improve ease of assembly.

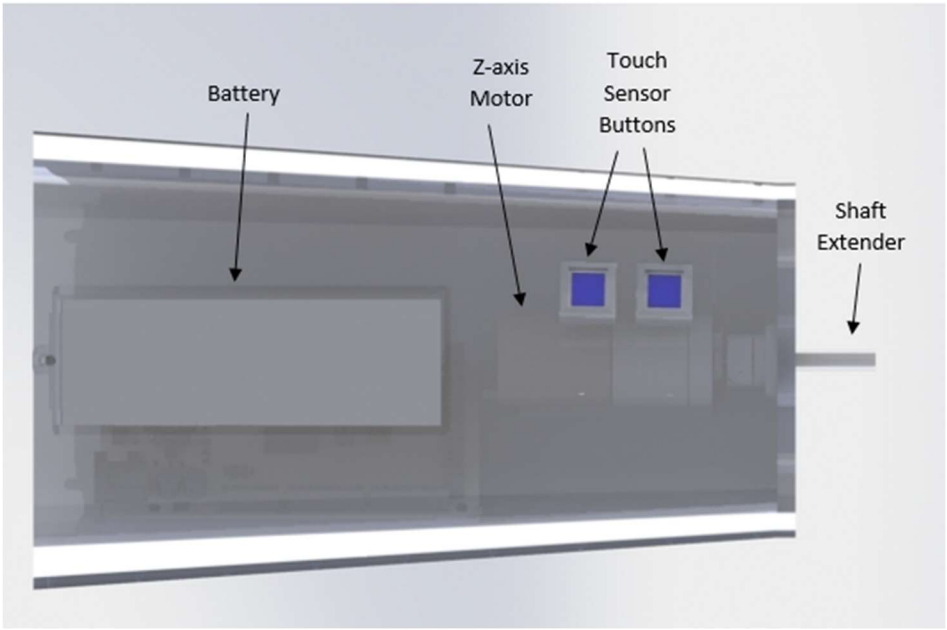

Figure 46: Forearm Subassembly Top View

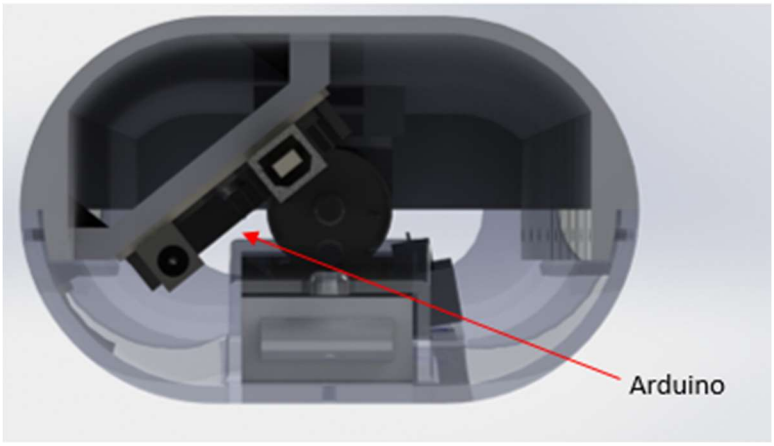

Figure 47: Forearm Subassembly End View

5.1.2 Fingers

The fingers needed few modifications between the first and second prototypes. The removal of the force sensor wire holes helped to reinforce the moving joint, however it left most of the wire exposed to the environment. This was not ideal for the final design, so a new wire hole was added to the top joint. As pictured in Figure 48 the hole routed the wires out the back of the top link, over the joint, and down into the bottom link.

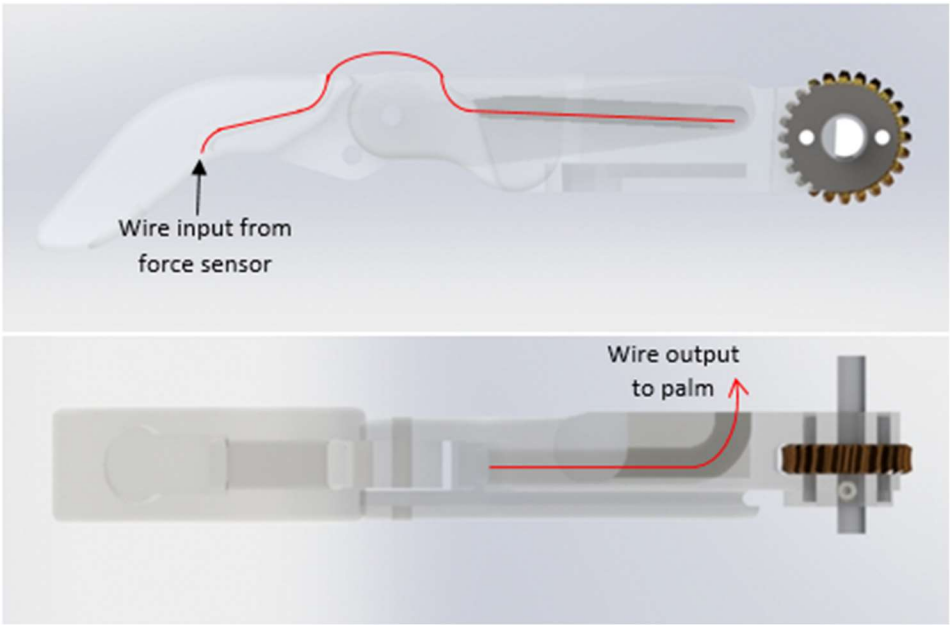

Figure 48: Final Prototype Finger with Wire Path

The force sensor slot was reduced to a 3 mm maximum depth, to allow the sensor more contact with object during grasping. A second force sensor was added to the bottom links of the index, middle, and ring fingers for feedback on smaller objects. Since the little finger cannot move independently and has minimal contact with objects compared to the other fingers, all of its force sensors were removed.

To reduce the slack in the system as the fingers rotated, the bottom shaft holes were modified to be D-Shafts. This guarantees the finger moves with the shaft with minimal backlash. The set-screws were kept for additional stability.

5.1.3 Palm

To look more anthropomorphic, the top and bottom covers of the palm were curved more than the previous design. This change, illustrated in Figure 49, modified the aesthetics without reducing usable inner space. A new cover was created to match the palm curves. This cover had holes for the thumb to rotate and two holes for the camera lens and IR sensor.

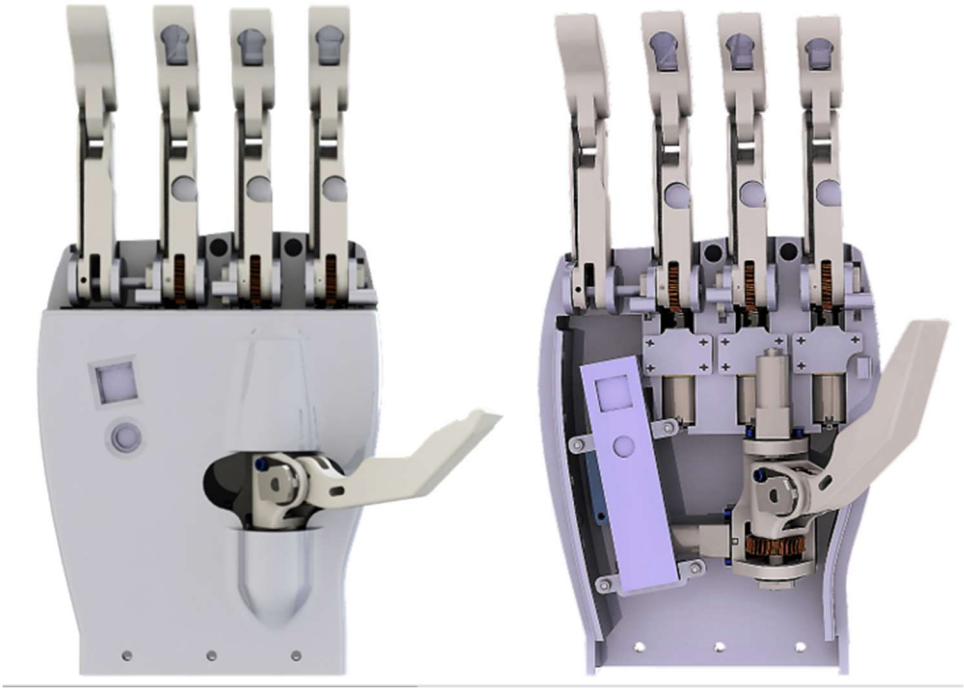

Figure 49: Modified Palm Case

As pictured, the bottom thumb motor was moved from the bottom of the joint to the top. This opened up more space in the palm, allowing the thumb to be moved downwards for improved grip poses. With the extra space at the bottom of the palm, the attachment area for the wrist was extended for added support.

The motor bracket holes were widened to fit heat-set inserts and flat head screws. The potentiometer cases were moved to more accessible locations for easier attachment. Each case was modified to cover half of the potentiometer instead of the full for easier alignment of the shaft with the hole. Pin holes were added to the knuckle for the linkages. The fingers were fully assembled in the CAD and all rotation was simulated to test range of motion and finger curl.

Due to the success of the side supports in the first forearm, this design was adopted for the new palm. The support columns were removed and a solid wall of plastic was created. This wall was just thicker than the inserts, so the material would not bend or warp as the inserts were placed.

5.1.4 Wrist

The wrist remained largely the same, however the top and bottom links were elongated: the top link to extend the connection between the palm and wrist, and the bottom link to set the motor down into the plastic. The latter extension allowed for a bigger gear on the x-axis motor to create a 2:1 gearing on the wrist. Since no other motor was small enough to fit within the compact wrist, a 2:1 gearing on the 1000:1 Pololu motor was the only option to increase torque. While the bigger, metal gear slows the rotational movement, the torque increase should be enough to hold up the palm.

The plastic around the bearings were thickened and widened to reduce cracking. On one side, a slot was made for the potentiometer. This slot was covered on three sides to restrict all possible movement. To accommodate this cover, the shaft must be placed through the other bearing.

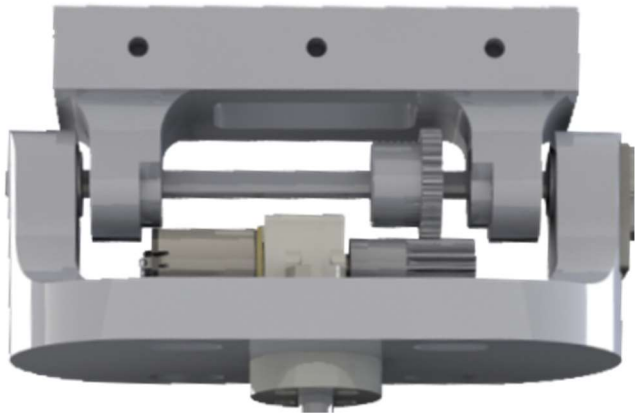

Figure 50: Updated Wrist Design

5.1.5 Forearm

Modifications to the forearm were focused on two main aspects: 1) making all wired components be contained on the same side of the arm to reduce excess wiring and make access easier and 2) change the z-axis wrist motor. In order for all electrical components to be on the same side, the Arduino had to be placed on its side to allow for protoboard slots to be placed directly beside the Arduino in the same half of the arm. Standing the Arduino up on its side was not ideal because it decreased stability and increased the overall inner arm dimension needed to fit that orientation. Instead, an angled platform was built extending from the inner forearm walls. This kept the Arduino fully supported while maintaining enough horizontal room for motor drivers to be placed on protoboards on the slots to the left. This design, shown in Figure 51, keeps the wires for all electrical components, aside from the battery, in the lower half of the arm.

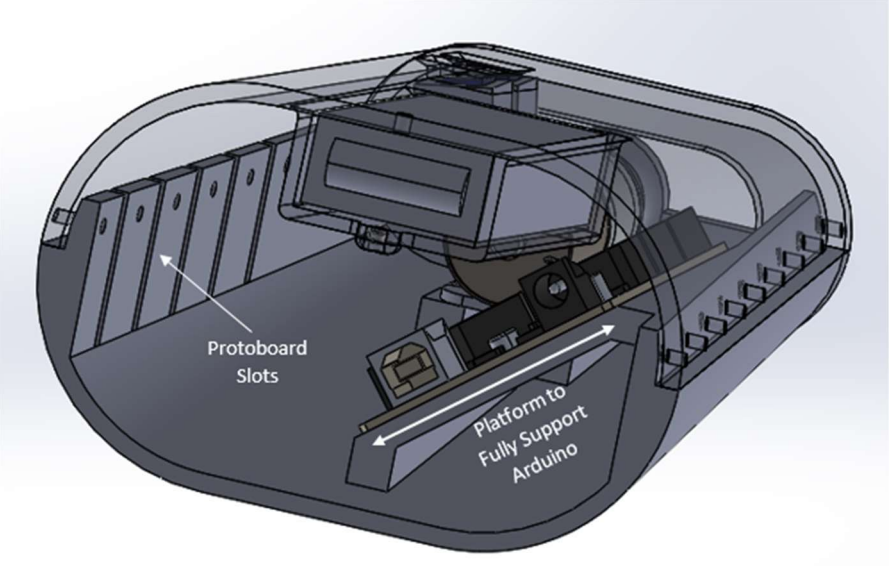

Figure 51: Forearm Redesign to Accommodate Wiring

Battery placement in the second prototype was once again kept along the forearm center to maintain an even weight distribution. Since one project goal was easy battery removal, a slot for the battery was created towards the forearm opening. When in use, the battery is secured by a screw that is threaded from the top of the arm down past the battery opening. When it comes time for the battery to be charged, the screw just needs to be removed so that the battery can slide out. This method, compared to the initial prototype which required the entire arm to be opened for battery removal, fits the goals of this project better since it allows for one-handed removal without the complete disassembly of the arm.

Changing the z-axis wrist motor, which is housed in the forearm, was the second large modification necessary for the final prototype. Securing the new motor in place within the arm, fitting the potentiometer, and extending the short 12 mm motor shaft to fit into the wrist were the challenges in this modification.

When discussing methods of extending the motor shaft, two potential designs were considered. The first, shown in Figure 52, used a 1:1 gear ratio to offset the motor and give the team the ability to choose any new desired shaft length. However, this design added more weight and moving parts to the overall assembly. It also increased the overall space needed between the forearm and wrist since space for the gears had to be considered. This design also relied on two screw mounting holes in the front face of the motor to support the entire motor weight and left the motor body completely unsupported. Potentiometer placement was also not ideal in this design, since the only possible spot would have been on the far side of the extended shaft behind the rotary bearing where it created interference with the motor face. Benefits to this design were that the rotary shaft the supports the hand and wrist would have been fully supported on either side and there wasn't the risk of a collar falling off or snapping as a result of bearing too much weight. However, this benefit did not outweigh the possible room for error that came with adding in more moving parts, so another design was modeled.

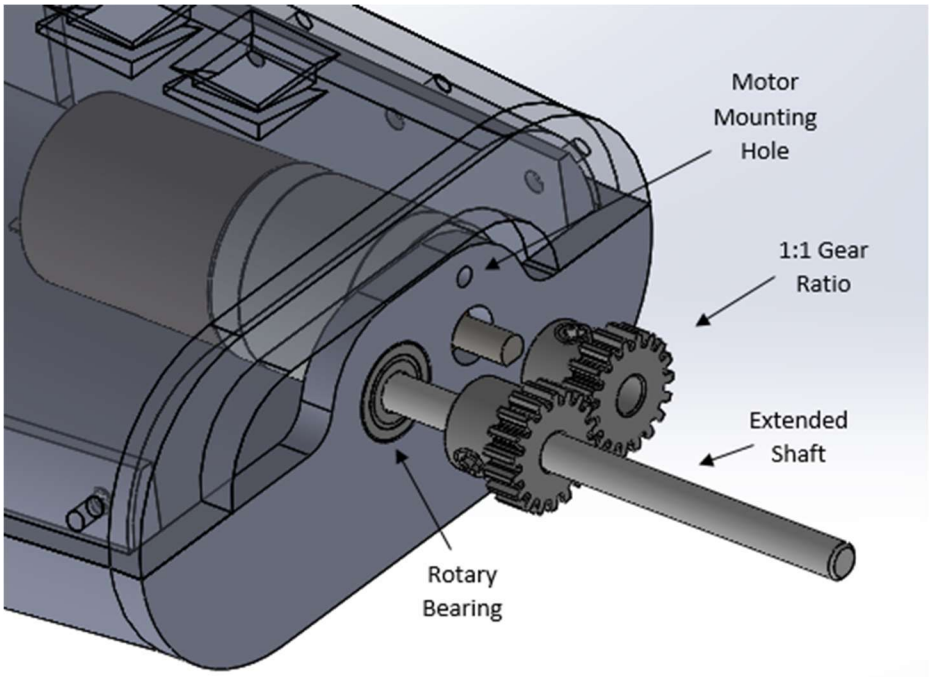

Figure 52: Design 1 - A 1:1 Gear Ratio

The second design, shown in Figure 53, uses a shaft extender as a more direct method of getting the shaft length required. This shaft extender is secured onto the motor drive shaft with a set screw and is one continuous part that then leads to a shaft extension. A key concern in using a shaft extender or shaft collar was that set screw connection points held more of a potential for breaking/slipping bearing a load. To provide more support for this collar, the motor was moved back into the forearm and a support collar was extended around the shaft extender. This then meant that the shaft was fully supported on either end and the weight of the hand and wrist was not supported to the motor shaft by a single set screw.

Since the motor was moved back from the front face of the forearm, connecting the motor directly to the forearm with screws was no longer viable. Instead, a motor mounting bracket from the motor supplier was utilized. This bracket connects to the front face of the motor, and then extends in an L shape to provide a user with multiple mounting holes along the length of the motor. To secure the motor to the forearm, the inner face was extruded up to meet the end of the motor plate so that the motor plate could be screwed into the forearm. Overall, this design was better at supporting the entire length of the motor while adding the necessary shaft length. This design also doesn't require any additional moving parts or a larger gap between the wrist and forearm.

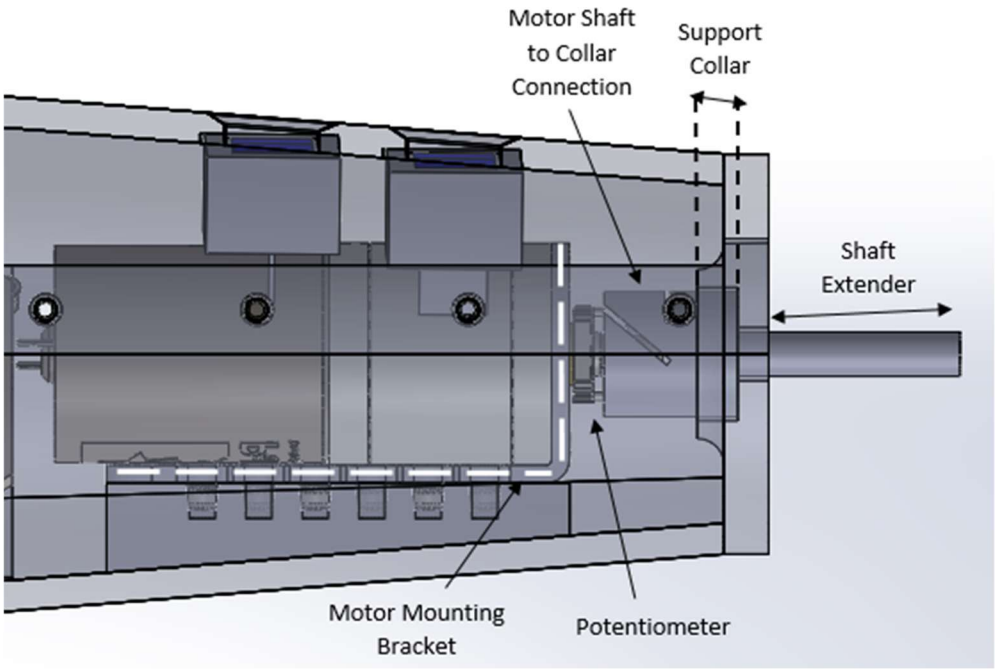

Figure 53: Design 2 - A Shaft Extender

The final aspect of the design was the potentiometer placement. Since it cannot be connected to the end of the shaft, the only other possible placement was at the base of the motor shaft before the collar. Since there was enough length to do this, that is where the potentiometer was placed.

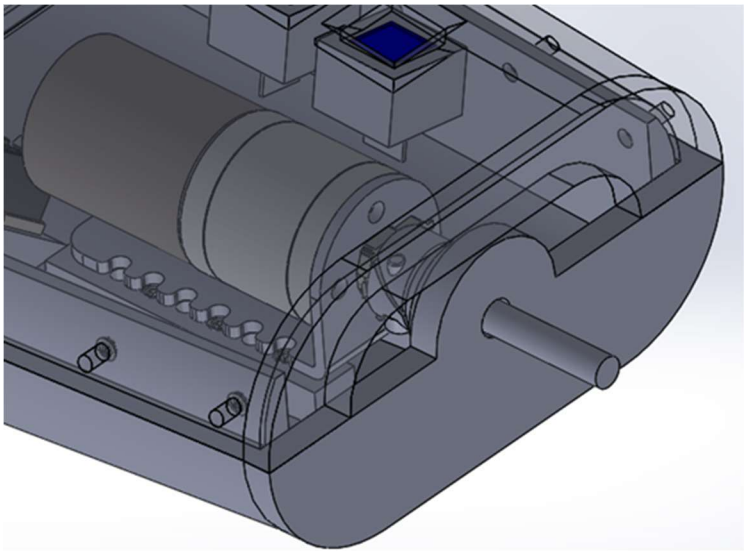

Figure 54: End of Forearm to Wrist Connection

These designs also preserve the ability to easily remove one half of the forearm. The front forearm face was redesigned so that the entire motor connection is confined to half of the assembly (Figure 54). This means that no motor disconnections will need to occur when opening the forearm. As shown in the figure, there are also spaces for wires to enter the forearm from the wrist on either side of the motor.

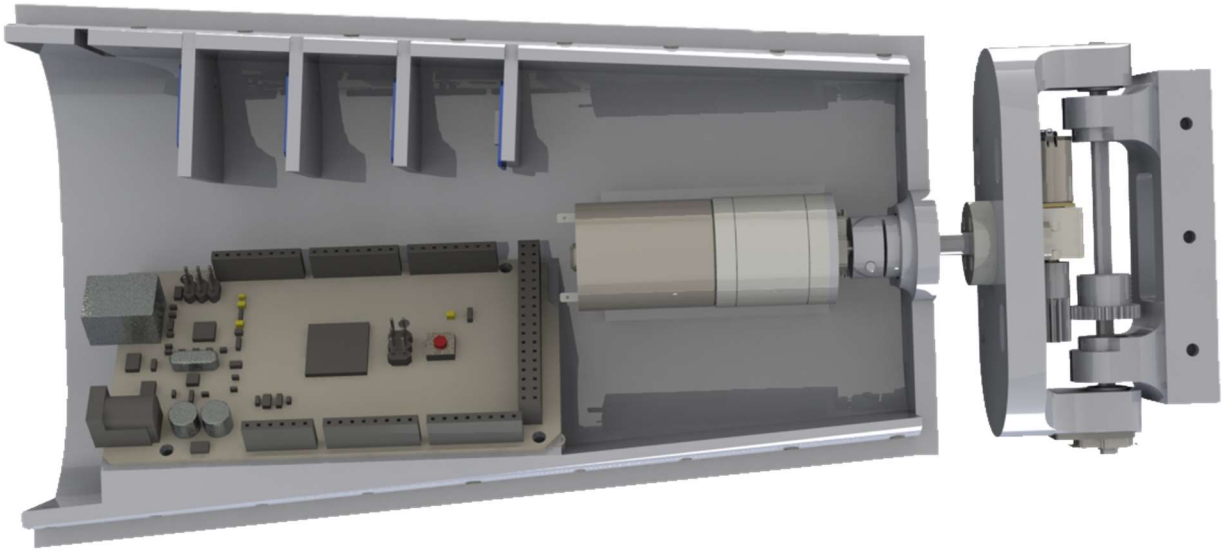

Figure 55: Updated Forearm and Wrist Assembly

5.2 Electrical

Due to magnetic fields produced by the motors, the IMU was placed 27 mm to the right of the center line running from the fingers to the wrist and in line with the center of mass. The protoboard sheets in the forearm were unnecessarily difficult, so these were replaced with 3 mm thick acrylic sheets. To compensate, the motor drivers were redone to have the wires soldered to the top instead of the bottom. The fully soldered motor drivers were attached to the acrylic with screws and placed in four of the forearm slots.

For organizing the wiring in the palm for the force sensitive resistors, the team decided to make a printed circuit board (PCB). This PCB was made by HK Weiku Information & Technology Co., Ltd (pcbway.com) consisted of seven voltage dividers. The force sensitive resistors were connected to the 5V Vcc supplied by the Arduino and 20 kΩ resistors were connected to ground. The analog input from the Arduino measured the voltage drop across the 20 kΩ resistors. The PCB can be seen in Figure 56.

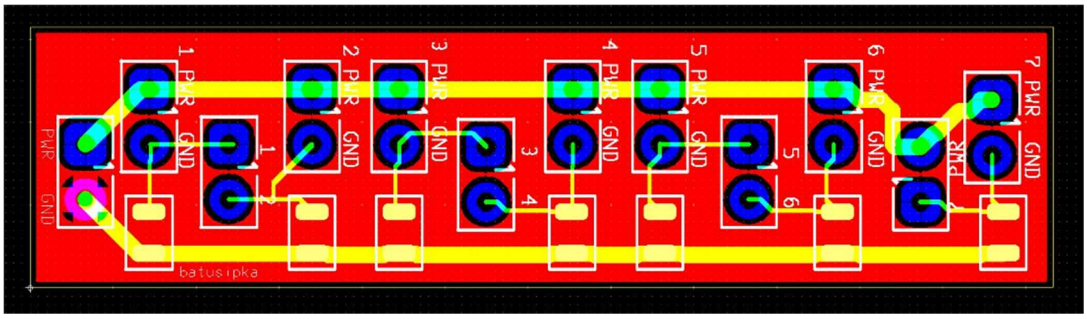

Figure 56: PCB for Force Sensors

The final electrical subsystem can be seen in Figure 57 below.

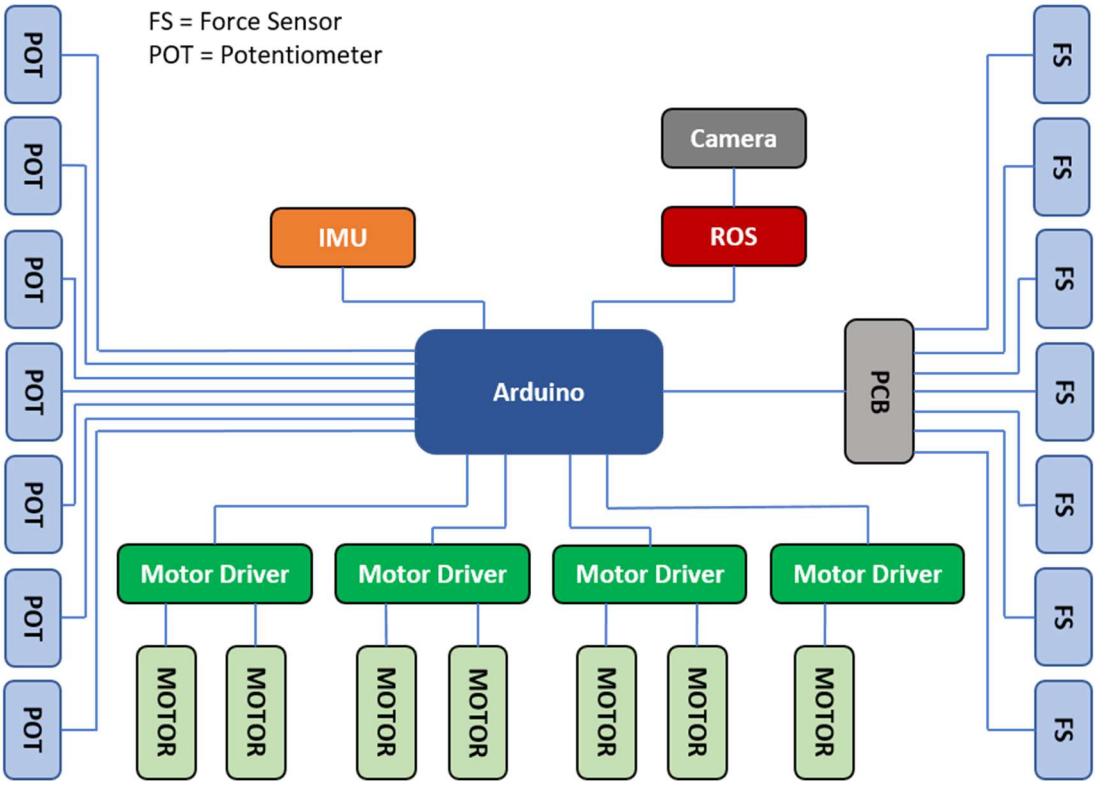

Figure 57: Electrical Subsystem for Final Prototype

The 11.1 V battery was not suitable for the motors and it would have caused overheating issues if Arduino got powered with it, so a 7.4 V battery was used for this design. While bigger, the battery is safer for testing and control. The chosen lithium polymer battery was a 2800 mAh 2-Cell Thunder Power RC ProLite X. This is the same brand as the previous 11.1 V used by Frankenhand and 7.4 V used by Paul Ventimiglia (Ventimiglia, P., 2012 and Merlin, M., & Sullivan, K., 2016).

5.3 Software

The main problem with the first prototype was reliability. The code was modified to better incorporate sensor feedback and smooth the movements as the joints rotate. Improved sensor feedback caused the previous code to slow down, as it takes more time to gather the data. This was solved by breaking the code into separate control loops for each rotation. The main loop was broken into three different modes: grasping, releasing, and self-balancing, these modes are summarized by the control flow in Figure 58.

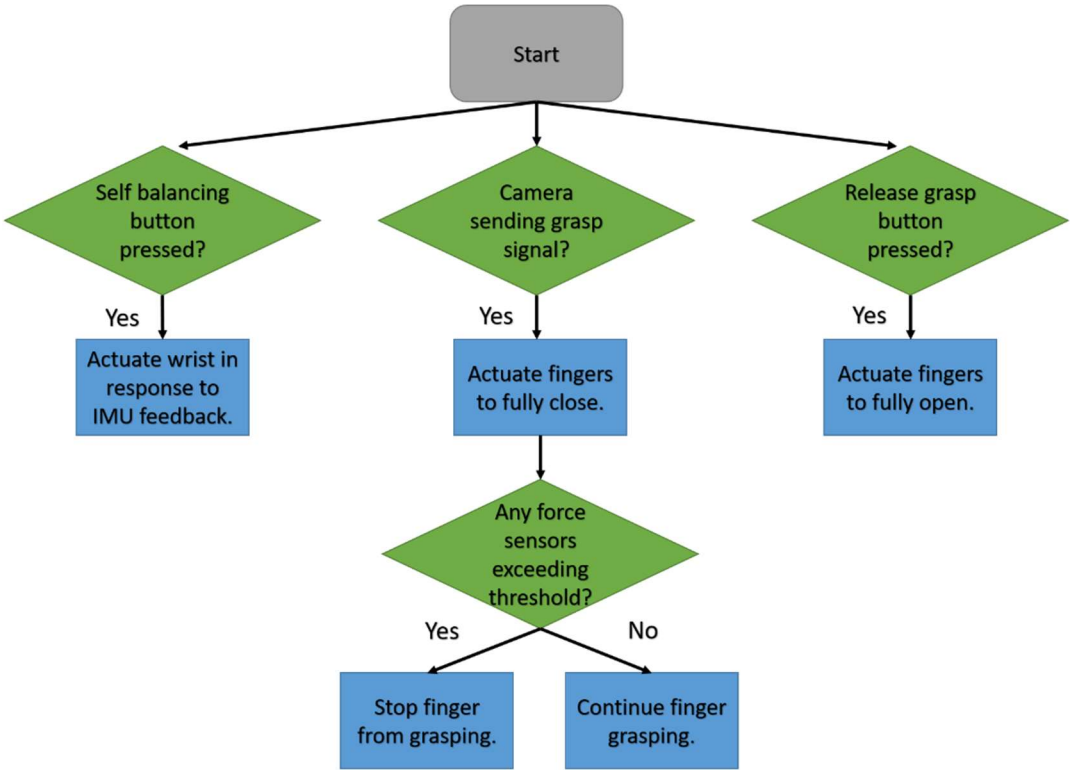

Figure 58: Control Flow

Grasping mode waits for a serial input from the camera. Once the hand received a signal to grasp, the fingers close to their preset target value. If the force sensor threshold is hit, meaning the finger is in contact with the object, the sensor sends feedback and the finger stops moving. If the object moves off the force sensor before the hand moves to release, the finger will begin moving until it reaches the target position or the force sensor regains contact. This allows the hand to get a firm grasp on the object, even if there is slippage.

For releasing mode, the hand waits for a press on left forearm touch button. This signal acts as an interrupt which sets the control to releasing mode, moving the fingers to their neutral open position.

If the right forearm touch button is pressed, the hand will enter self-balancing mode. This button activates the wrist and forearm motors. The IMU reads the initial angles in the x- and z-axes and sets those angles as the target position for the control loop. When the hand moves in either direction, the motors compensate in that direction to ensure the palm maintains its initial orientation.

The sensor readings were conducted using a 500 Hz timer interrupt and the control loop with a 1 kHz interrupt.

5.4 Vision

A number of factors needed to be considered before choosing a camera. The camera needed to collect data in 3D dimensions, as depth was a major factor in Dexter's autonomous capabilities. The camera also had to be smaller than 94 x 42 mm to fit within the allotted palm space, with an ideal thickness of 8.5 mm or less. This severely limited the number of feasible options, as most 3D cameras are quite large or require an onboard processor. These concerns, as well as budget and time, left two possible camera options: The

BlackBird 2 and the CamBoard pico flexx. These cameras, along with the testing and analysis was provided by Aditya Gupta, a WPI Masters Student.

The first camera considered was a 3D FPV camera The BlackBird 2, shown in Figure 59 below. This camera cost $180, weighed 23 g, and had an input voltage range of 5 to 15 V. To get depth information, the camera uses a real-time stereoscopic analog video with a 5.8 GHz telemetry. The device measured 59 x 28 x 27 mm, which fits in the x and y directions, but is over three times thicker than the ideal thickness. Due to the stereo images, a FPV video transmitter is also required in the forearm.

Figure 59: The BlackBird 2 (3D FPV camera The BlackBird 2, n.d.)

The next camera considered was a CamBoard pico flexx. This device has a built-in infrared (IR) sensor to detect the distance to surrounding objects. The camera has a range of 0.1 to 4 m and a 62 x 45-degree field of view (Reference Design Brief CamBoard pico flexx, n.d.). The device creates a point-cloud of the surrounding objects, giving the prosthetic hand the x, y, and z locations of any object it is trying to grasp. This camera proved ideal for the given task, and required no additional hardware, so it was attached to the bottom cover of the palm. However, since the Arduino Mega does not have enough computational power to process 3D images, the camera needed a USB cable for data transmission to an external computer. This camera can be seen in Figure 60.

Figure 60: CamBoard pico flexx (picoflexx blog, n.d.)

The images from the pico flexx are processed in ROS. The initial point cloud, Figure 61, is filtered to eliminate background objects, large flat surfaces (walls, tables, etc.), and noise. The filtered image is then used to determine the general shape and size of the object. The object shape is classified into one of three distinct categories: cube, sphere, or cylinder.

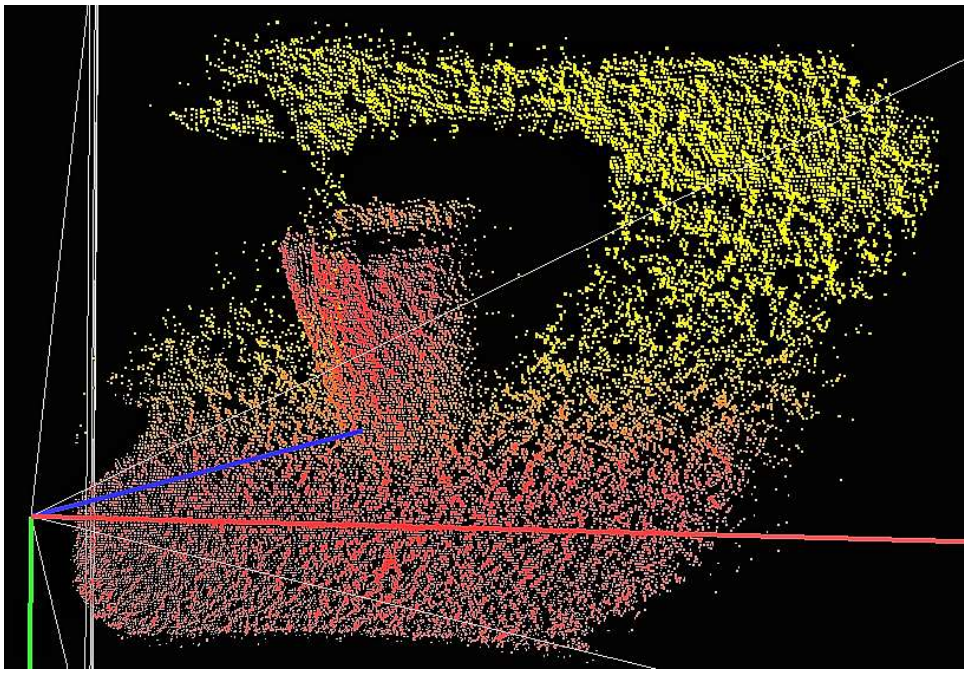

Figure 61: Point Cloud of Cup Taken by CamBoard pico flexx

6. Testing

The overall testing for the second prototype was broken into two parts: individual components and full assembly. As each component was assembled, it was tested to ensure all joints and sensors were working as expected.

Each finger was run individually to measure the maximum and minimum potentiometer values. During this phase of the testing, there were some problems with meshing of gears. The worm gears and circular gears would mesh correctly as the finger moved to a closed position, but skipped as they opened. This was solved by placing strips of paper as spacers under each finger motor to push it up into the worm gear. Once all of the fingers were modified and able to actuate separately, they were run simultaneously to measure the time response. This information was used to tune the P-values in the control code. Figure 62 illustrates the P-control algorithm running in real time. The finger goes to the position 525 (ADC units) without any significant undershoot or overshoot. This graph proves that P-control is enough for the fingers to move to static desired positions.

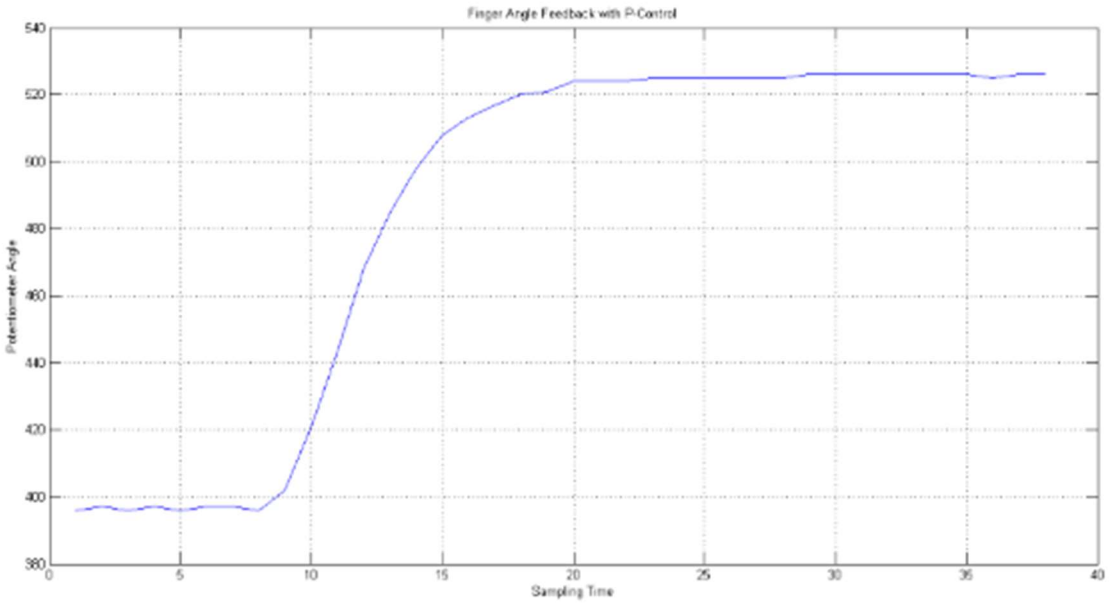

Figure 62: Finger Angle Feedback with P-Control

Figure 63 shows the force sensors changing its output voltage due to applied force. It is proved that with a normal force of between 0.392 N (40 grams) to 1.765 N (180 grams) uses 72% of the voltage range.

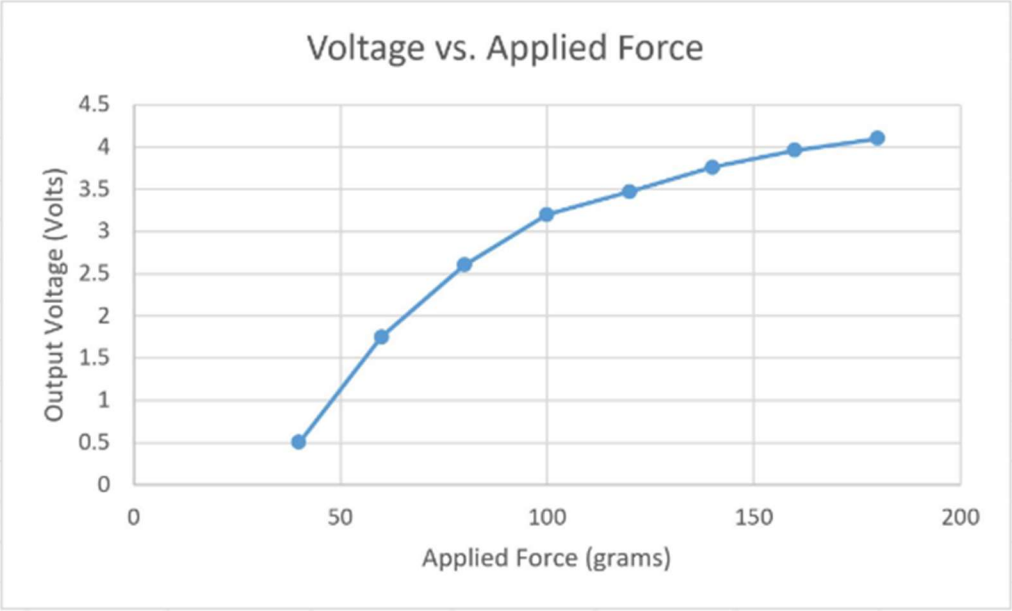

Figure 63: Voltage vs. Applied Force Graph

While testing grasp poses, a stationary object was placed on a flat, empty surface to eliminate interference in the camera data. As the hand moved towards the object and the distance threshold was met, the fingers all moved correctly to the target value and stopped all movement if the force sensor threshold was met. However, the location of the thumb force sensor was too high for some object shapes. The test can be seen in Figure 64.

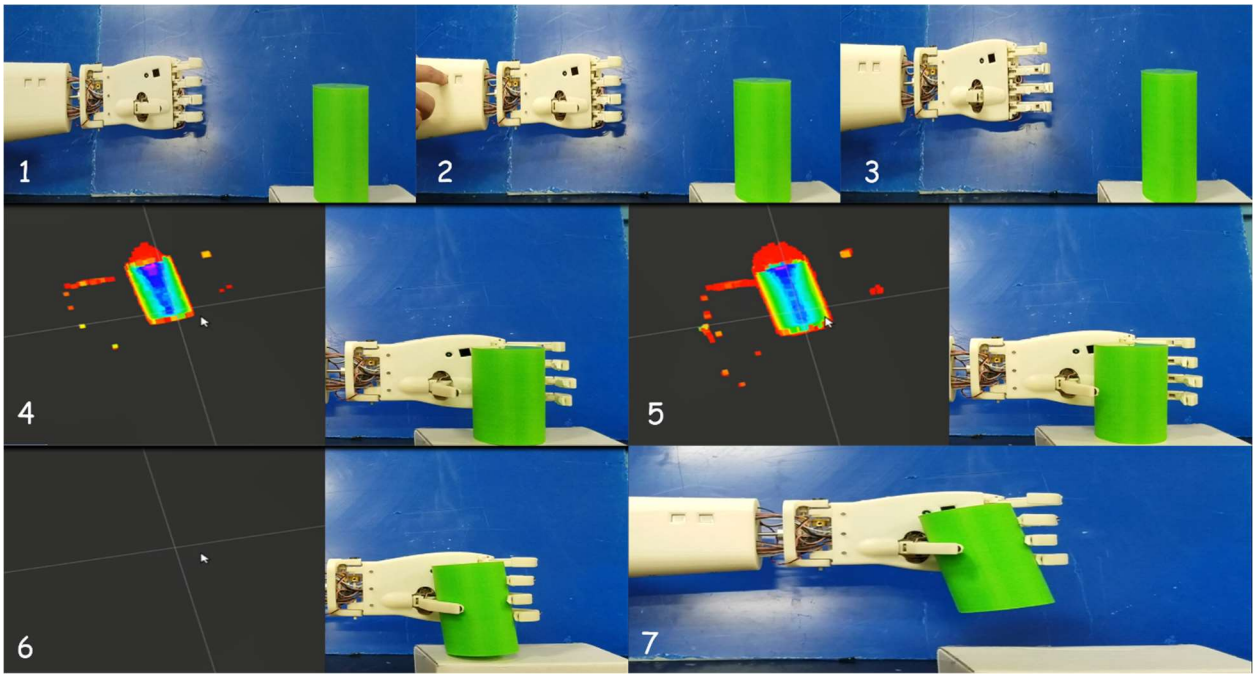

Figure 64: Cylindrical Object Grasp with Camera Feedback

In the first picture of the Figure 64, Dexter is in closed grasp position. Second picture demonstrates the touch sensor press to set the fingers to an open position. The fingers going to the open position can be seen in the third picture. Picture 4 illustrates the point cloud data from the camera when the hand is approaching the object. In picture 5, the hand receives the close grasp signal from the camera to start the grasping process. Information exchange between the Arduino and pico flexx was conducted with serial communication. Once the hand moved into the critical distance threshold, the camera sent a signal to begin grasping. The camera code would get stuck occasionally or process the information too slowly, causing the signal to be delayed. However, the camera testing worked 95% of the time.

It can be seen in the sixth picture that there is no point cloud left since the camera is too close to the object and already grasped it. This is where the force sensor feedback takes control of the movement; the fingers will keep grasping until their force sensors get a good contact with the object or they reach them. In picture 7, the cylinder begins to slip out of the hand. The force sensors were able to detect that an insufficient amount of force was being applied to the object. Once the force fell below the threshold, the fingers began grasping firmer, saving the object from falling. During this test, the thumb force sensor did not make contact about 10% of the time, causing the finger to move into the part rather than stopping at the correct location.

To test Dexter's ability to grasp various shapes and sizes, the cylinder was replaced with a cube. This test was conducted using the two touch buttons, rather than camera feedback. The right button activated grasping mode, while the left signaled the hand to release, see Figure 65.

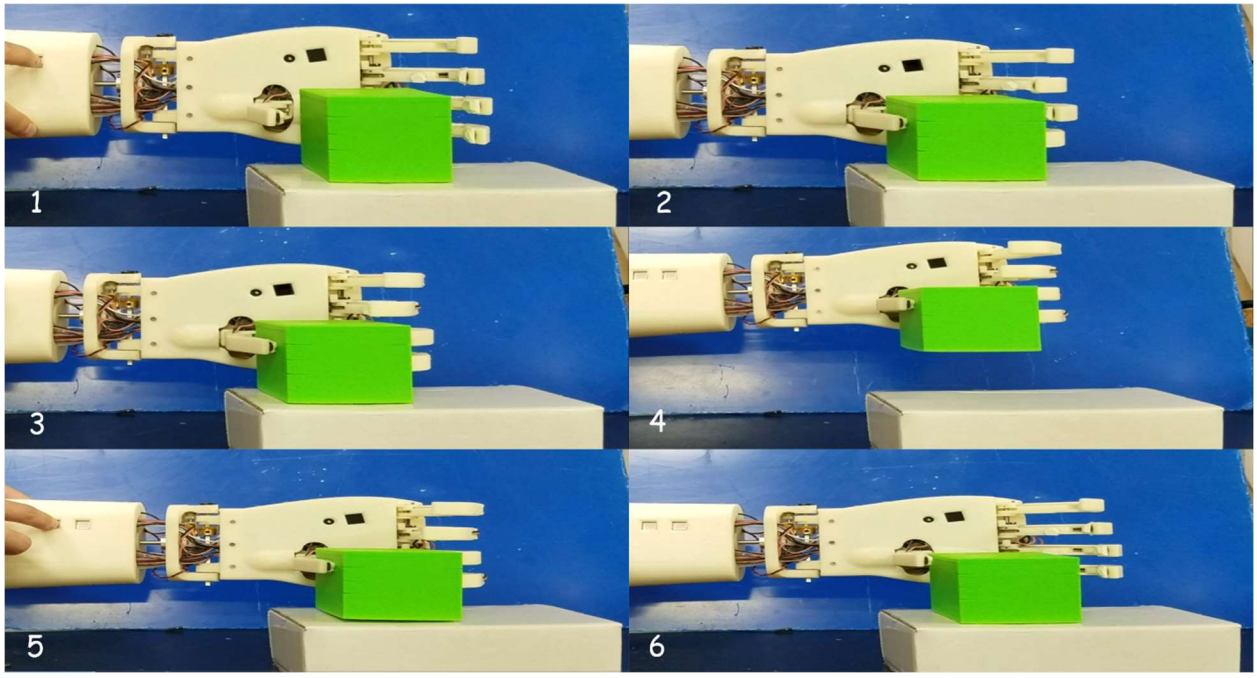

Figure 65: Grasping a Cube

Picture 1 in Figure 65 demonstrates the open position and the button press to close the grasp. In picture 2, the fingers all begin actuating together to grasp the cube. Picture 3 illustrates the force sensors in the thumb, index and middle finger making contact with the surface. The ring finger did not make contact, so it continued moving until it reached its closed position. In picture 4, Dexter was able to lift the object and

maintain the appropriate grasping force. Once the object is ready to be placed back on the table, picture 5, one button press initiates the release, illustrated in picture 6.

The next test was self-balancing mode. Before the wrist was attached to the assembly, the x- and z-axis wrist motors were tested individually. The P-values in the control loop were tuned manually so the wrist and forearm would not over- or under-shoot during movement. Both motors correctly maintained their orientation in the x- and z- directions with little-to-no jerky movements, so the wrist was attached to the full assembly. Since there were only two degrees of freedom, the wrist failed to work properly if the y-axis changed. This was unavoidable with the current design, so the testing of the wrist was deemed complete. Figure 66 shows the steps that are completed in the self-balancing test.

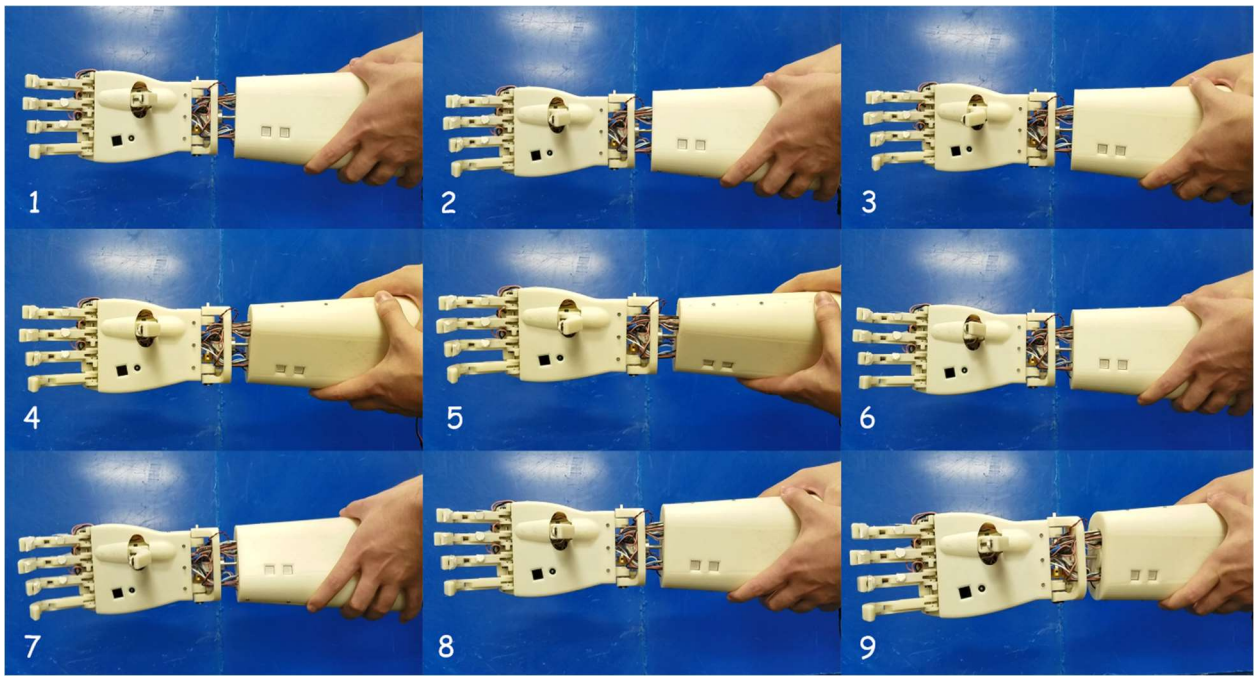

Figure 66: Self Balancing Mode Test

Picture 1 demonstrates the initial position of the hand. The hand was held by one of the team members to move the forearm in z and x directions respectively. It is expected that the forearm joint compensates for the z-axis rotations and the wrist joint compensates for the x axis rotations. Picture 2 shows a slight turn in +z direction and the forearm seems like it is working properly. After returning to the initial orientation, picture 3, the forearm was rotated in the –z direction and as seen in picture 4, the hand stayed upright. Picture 5 illustrates a more drastic rotation in the –- direction. The hand was also tested for rotation about the x-axis. Figure 9 shows that if the hand was moved towards in the +x direction (out of the page), the wrist will compensate by moving in the –x direction (into the page). Movement in the –x direction was also tested, but it not illustrated in Figure 65.

7. Results

Dexter has the ability to firmly grasp objects ranging in size from 10 to 90 mm, as shown below in Figure 67. This analysis was done by utilizing CAD to grasp cylinders with increasing diameters and placing the normal force vectors accordingly. If the force vectors crossed and pointed towards the hand, it was assumed the object could be grasped. Once the force vectors were no longer crossing and became parallel, as they did in the 100 mm screen of Figure 67, it was assumed that the hand would be unable to continue grasping the object. Since this is preliminary grasp analysis done using CAD, there is the potential that Dexter may be able to grasp objects of a larger diameter of a different shape, especially considering friction forces at contact points.

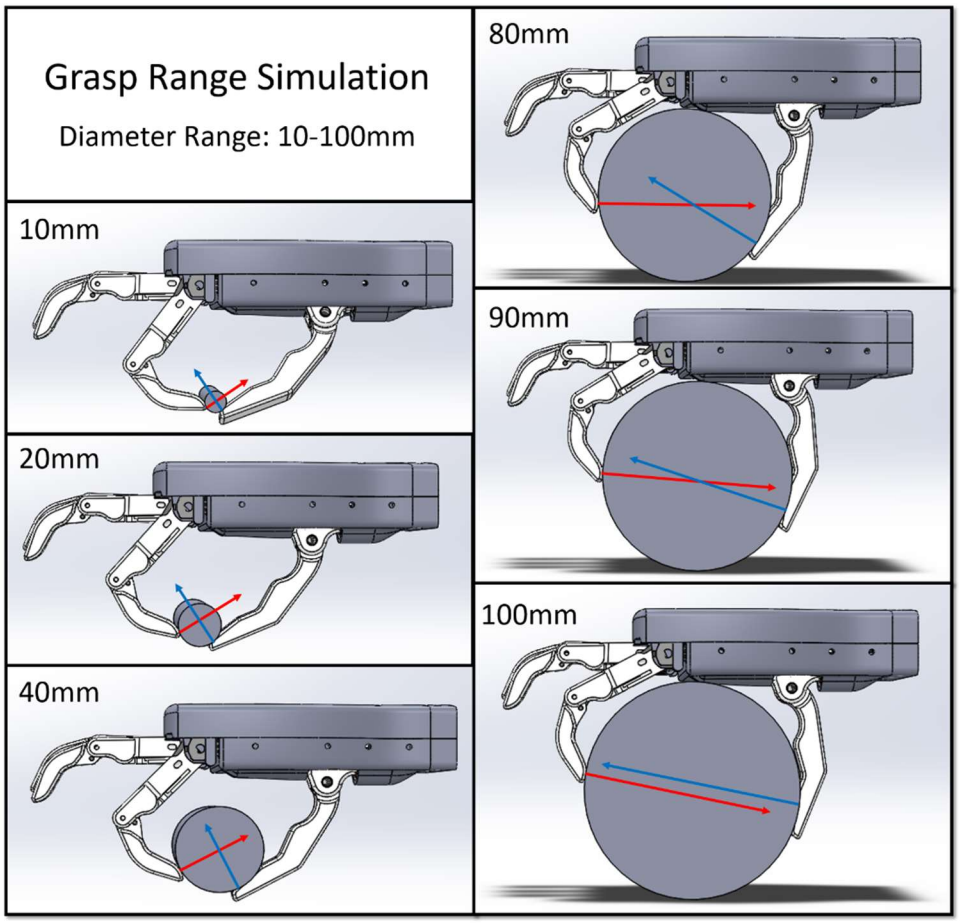

Figure 67: Graspable Range Simulation in SolidWorks

Dexter can achieve ten different poses, as described by BeBionic (bebionic3 technical information, 2012). These poses are tripod, pinch, power, active index, finger point, mouse, precision open and closed, open palm, and relaxed hand. This number, second only to I-limb and BeBionic, is largely due to the two degree of freedom thumb, which can roll and pitch to achieve a larger variety of poses. This thumb opposition is something not all commercial hands have, which is why it is generally only seen on the high cost, high functioning hands such as I-limb and BeBionic.

While the max grip force was not measured, Dexter is comparable on all other fields to the leading prosthetic hands, outperforming the others on feedback, battery life, and price. This comparison is

outlined in Table 6 below. The total weight of the device is 1,040 g, 710 g lower than the objective. The weight of the hand and wrist alone is 530g and the wright of the forearm, with a battery in place, is 510g.

Table 6: Comparison of High-Functioning Prosthetics

Hand	Price ($)*	# Grips	Weight	Max Grip Force**	Speed of Finger Curl	Battery Life (mAh)	Force Feedback	Visual Feedback
Michelangelo	75,000	7	420g	70N	325 mm/s	1500	No	No
I-limb ultra	17,000	14	500g	100N	1.2 s	2000	No	No
BeBionic	11,000	14	700g	140N	1 s	2200	Yes	No
Ada	700	5	380g	49N	N/A	N/A	No	No
Dexter	**1,425*** **	**10**	**530g**	**N/A**	**1.8 s**	**2800**	**Yes**	**Yes**

*in some cases estimates based upon research, **for power grip, ***for prototype cost of parts

8. Conclusion

The team was able to successfully design and create a prosthetic hand, wrist, and forearm to meet the required project objectives. Dexter is an anthropomorphic device that is integrated with object recognition and can autonomously grasp objects in its environment. Dexter also has force, angle, and orientation feedback to allow for the successful gripping of objects with varying harnesses and is able to maintain a self-balancing orientation.

The only objective that the team was unable to test was 2a, which was holding a cup of water and not spilling the contents. Although we were unable to test this objective given time constraints, we were able to validate the different components necessary to complete this task. Dexter has a grip range necessary for holding a cup of water and is able to successfully self-balance on its own, so if time permitted we expect Dexter would have been successful in satisfying this objective.

Dexter is a high-functioning, low-cost device. Once Dexter was completed, the functionality matrix was updated to include this device. Force feedback and visual feedback were added to the matrix functionality scoring categories (grip, force, weight, wrist, power, battery life) used previously. Based upon these categories, an updated matrix was created as shown in Appendix C: Final Functionality Ratings. A few assumptions were made in creating these tables, namely the maximum grip force. There was not enough testing to provide Dexter with a maximum grip force, so it was assumed that the force would be greater than that of the hooks and tendon powered hands, but still possibly lower than other hand prostheses on the market, thus Dexter was given a rank in the middle of the range. This functionality matrix resulted in the overall functionality ratings shown in Table 7.

Table 7: Final Functionality Ratings

DEVICE	FUNCTIONALITY RATING	PRICE (USD)
AXON HOOK	14	15,000
GRIP 5 EVOLUTION PREHENSOR	9	1,200
MICHELANGELO HAND	22	75,000
I-LIMB ULTRA	31	17,000
BEBIONIC	32	11,000
ADA HAND	14	700
DEXTER	27	1,425

These functionality ratings were once again plotted against cost. The Michelangelo Hand was removed from this plot since it's high cost made it a large outlier within the data. In this updated functionality matrix, the mean value that was set as the minimum for a high functioning device was a 21.2. Thus, as shown in Figure 68 Dexter fulfilled the need of a high-functioning, low-cost prosthetic with a rating of 27 and a price of $1,425. As this price is calculated based only the cost of parts while the other devices are market price, it is important to recognize that should Dexter be sold, the cost will increase. An estimation of this cost for a 20% profit margin is $1,707 – so Dexter can be profitable and still be kept at a market price of under $2,000.

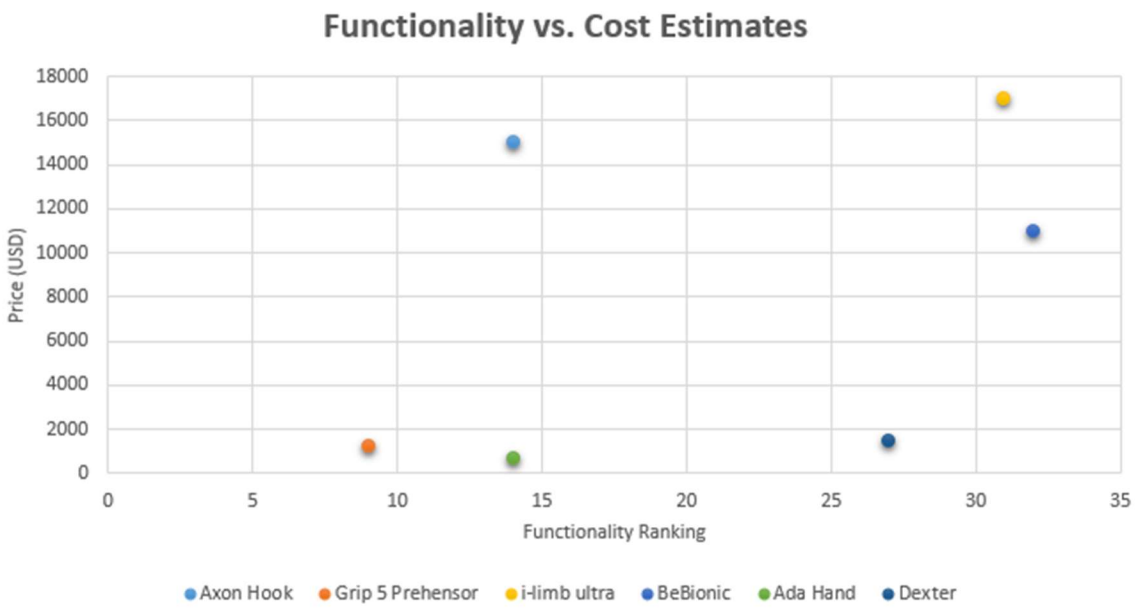

Figure 68: Updated Functionality vs. Cost Graph

Using the functionality ranking and the associated cost, a metric was created to show the relationship between functionality and cost. This metric was device functionality divided by the price. In this method, a higher value would mean that there is a high level of functionality for the devices cost. As shown in Figure 69 below, Dexter and the Ada Hand have the highest values. Despite the Ada Hand's higher rating, this device has limited functionality, as that is what is producible at such a low cost. Since Dexter is high functioning and still is only 0.001 away from having the same value as the Ada hand, it can be concluded that Dexter successfully bridged the gap and is an example of a high functioning, low cost device.

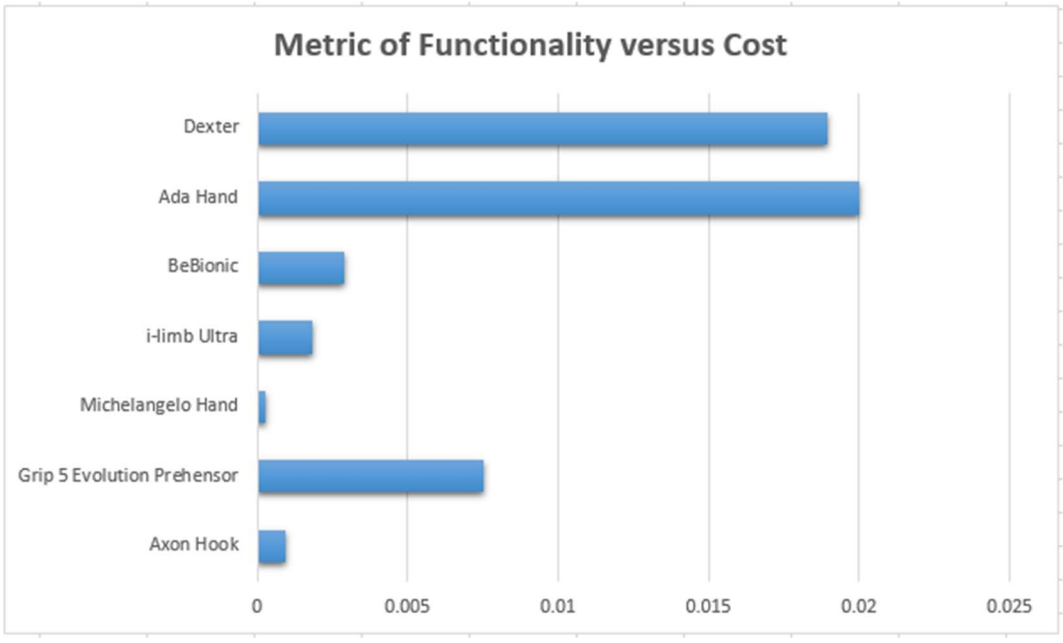

Figure 69: Metric of Functionality vs. Cost

8.1 Research Applications

Dexter is a one-of-a-kind prototype for prosthetic, imagery, and path planning research. The CAD model has been turned into a movement simulator, in which any object can be placed in front of the palm and device will determine the best movement to grasp. This simulation was developed at WPI Soft Robotics Lab by a PhD student (Selim Ozel) and will be used to conduct machine learning for grasping arbitrary objects in collaboration with Northeastern University and Harvard Medical School.

The CamBoard pico flexx will continue to be integrated and improved for research relating to object recognition, learning, and classification. This research will be conducted by PhD and MSc students at WPI Soft Robotics Lab.

8.2 Future Recommendations

The primary recommendation for future production of Dexter is to create an attachment to the user's residual limb. This component was out of the scope of this project, however, it is necessary if this device ever reaches the market. The forearm was designed to be compact enough in size to allow for this limb attachment. The connection is critical should this product go to market in the future.

The second recommendation for Dexter is to integrate myoelectric sensors to the limb attachment. In combination with the current Dexter sensors, myoelectric capabilities would allow the hand to be both autonomous and controllable by the user. The addition of these sensors would eliminate the need for one of the touch sensors on the forearm, as muscle movement could send the signal to grasp and release an object. The second button could be eliminated if a different muscle movement, one not associated with grasping or releasing, initiates self-balancing mode. This integration would give more independence and functionality back to the user, as all movements could be controlled without input from the other limb.

The last recommendation is a redesign of the wrist. Due to budget and time constraints, the wrist was only designed for two degrees of freedom: x and z. This made full functionality of self-balancing mode nearly impossible, as the hand could not correct for movement in the y-direction, leading to oscillations or failure. A three-dimensional wrist joint would eliminate this problem and provide a more human-like rotation for the user.

9. Works Cited

3D FPV camera The BlackBird 2. (n.d.). Retrieved from FPV3DCAM website: <http://fpv3dcam.com/products-fpv3dcam/the-blackbird2-3d-fpv-camera.html>.

3-D Point Cloud Processing. (n.d.). Retrieved from MathWorks website: https://www.mathworks.com/

Ada V1.0-Datasheet. (2016, January). Retrieved October 11, 2016 from OpenBionics website: www.openbionics.com .

Additive Manufacturing Infographic. 3D Hubs. Retrieved December 7, 2016 from: https://www.3dhubs.com/talk/thread/additive-manufacturing-infographic.

Adult Grip 5 Evolution Prehensor. Retrieved October 11, 2016 from TRS website: http://www.trsprosthetics.com/product/grip-5-evolution-prehensor/.

AM Basics. AMazing. Retrieved December 7, 2017 from: http://additivemanufacturing.com/basics/.

AxonHook. Retrieved October 11, 2016 from Ottobock website: https://professionals.ottobockus.com/media/pdf/13213B_AxonHook_Spec_Sheet.pdf .

bebionic3 technical information. (2012). Retrieved from BeBionic website: http://bebionic.com/distributor/documents/bebionic3_technical_information_-_Lo_Res.pdf

BeBionic3 Tech Manual. (2013). Retrieved October 11, 2016 from Steeper website: http://bebionic.com/distributor/documents/bebionic3_Tech_Manual_web.pdf.

Billock, J. (1986). Upper Limb Prosthetic Terminal Devices: Hand Versus Hooks. *Clinical Prosthetics and Orthotics,* 10(2), 57-65.

Body Segment Data. ExRx.net. Retrieved from http://www.exrx.net/Kinesiology/Segments.html.

Borrmann, D., & Elseberg, J. (n.d.). [Point Cloud of City Center Bremin]. Retrieved from http://kos.informatik.uni-osnabrueck.de/3Dscans/

Bowers, R. (2014, December). Prosthetic Devices for Upper-Extremity Amputees. *Amputee Coalition of America*.

Budziarek, M.B., Pureza Duarte, R.R., Barbosa-Silva, M.C. (2008). Reference values and determinants for handgrip strength in healthy subjects. *Clinical Nutrition, 27*:357-362.

Buryanov, A. & Kotiuk, V. (2010) Proportions of hand segments. *International Journal of Morphology, 28(3)*:755-758.

Casley, S., Choopojcharoen, T., Jardin, A., & Ozgoren, D. (2014, April). *IRIS HAND: Smart Robotics Prosthesis*. Worcester Polytechnic Institute.

Cross and Roller Universal Joint. (n.d.). Retrieved from Integrated Publishing website: http://constructionmanuals.tpub.com/14273/css/Cross-and-Roller-Universal-Joint-179.htm

Edwards, R., Lafontant, K., Sujumnong, N., & Wormley, J. (2015, April). *Vision-based Intelligent Prosthetic Robotic Arm*. Worcester Polytechnic Institute.

Fitting Your Prosthesis. (2015). Retrieved October 12, 2016 from Hanger Clinic website: http://www.hangerclinic.com/limb-loss/resources/what-to-expect/fitting/Pages/default.aspx.

I-limb ultra Clinician Manual Issue 2. (2013, March). Retrieved October 11, 2016 from Touch Bionics website: http://www.touchbionics.com/sites/default/files/i-limb_ultra_clinician_manual_issue._2.pdf.

Inspector General. (2012). *Healthcare Inspection Prosthetic Limb Care in VA Facilities* (Rep. No. 11-02138-116). Washington, DC: Department of Veterans Affairs Office of Inspector General.

Limb Loss Statistics. (n.d.). Retrieved October 12, 2016, from Amputee Coalition website: http://www.amputee-coalition.org/limb-loss-resource-center/resources-by-topic/limb-loss-statistics/limb-loss-statistics/#1

McGimpsey, G., & Bradford, T. C. (2008). Limb prosthetics services and devices. *Bioengineering Institute Center for Neuroprosthetics, Worcester Polytechnic Institute*.

Merlin, M., & Sullivan, K. (2016, April). *Frankenhand: An Intelligent Prosthetic*. Worcester Polytechnic Institute.

Michelangelo Brochure. Retrieved October 11, 2016 from ottobock website: http://www.ottobockus.com/media/local-media/prosthetics/upper-limb/michelangelo/files/michelangelo-brochure.pdf.

Murphy, Max. *3D Printing Tradeoffs and Optimization*. SKMurphy. Retrieved December 7, 2016 from: http://www.skmurphy.com/blog/2015/08/08/3d-printing-tradeoffs-and-optimization/

picoflexx blog. (n.d.). Retrieved from http://pmdtec.com/picoflexx/blog/tag/pico-flexx/

Ray, S. (2015, August 10). Essentials of Machine Learning Algorithms (with Python and R Codes) Retrieved October 11, 2016, from Analytics Vidhya website: http://www.analyticsvidhya.com/blog/2015/08/common-machine-learning-algorithms/

Reference Design Brief CamBoard pico flexx. (n.d.). Retrieved from http://pmdtec.com/picofamily/

Retrieved October 11, 2016, from EE Times website: http://www.eetimes.com/document.asp?doc_id=1279404

Russell, S., & Norvig, P. (Eds.). (2010). *Prentice Hall Series in Artificial Intelligence: Artificial Intelligence: A Modern Approach* (Third ed.). Upper Saddle River, NJ: Prentice Hall.

Semig, P., & Wells, C. (2012, February 8). [A Current Sensing Tutorial--Part 1: Fundamentals].

Townsend, K. (n.d.). Adafruit_BNO055 [Computer program]. Retrieved from https://github.com/adafruit/ Adafruit_BNO055

Ventimiglia, P. (2012, April). *Design of a Human Hand Prosthesis*. Worcester Polytechnic Institute.

Ziegler-Graham, K., MacKenzie, E. J., Ephriam, P. L., Travison, T. G., & Brookmeyer, R. (2008). Estimating the Prevalence of Limb Loss in the United States: 2005 to 2050. *Archives of Physical Medicine and Rehabilitation*, *89*(3), 422-429. http://dx.doi.org/10.1016/j.apmr.2007.11.005

10. Appendices

Appendix A: Cost of Initial Prototype

Item	Quantity	Amount	Total
Resistive Force Sensor 0.04-4.5 lbs	5	10.97	54.85
Rotary Potentiometer	7	0.50	3.50
1000:1 Micro Metal Gearmotor	6	23.95	143.70
Motor with Gearbox	1	21.95	21.95
Breakout Board 9-DOF IMU BNO055	1	34.95	34.95
Black-Oxide Socket Head Screw, 2-56 Thread, 1/4" Long	1	6.43	6.43
18-8 Stainless Steel Phillips Flat, 2-56 Thread, 1/4" Long	1	3.94	3.94
Arduino Mega 2560	1	37.49	37.49
Breakout TB6612 1.2A Motor DVR	4	4.95	19.80
Heat-Set Insert for Plastics, 2-56 Thread, 0.115" Long	1	9.67	9.67
Ball Bearing, 5/16" OD, 68000 rpm Max Speed	2	15.35	30.70
Plastic Gear - 14-1/2 Degree Pressure Angle	2	7.51	15.02
Worm Gears (8 total)	1	56.00	56.00
11.6 V Battery	1	29.99	29.99
3D Printed Palm and Fingers - ABS	1	90.32	90.32
3D Printed Wrist and Forearm - ABS	1	111.00	111.00
		Total	**669.31**

Appendix B: Cost of Final Prototype

Item	Quantity	Amount	Total
Resistive Force Sensor 0.04-4.5 lbs	7	10.97	76.79
Rotary Potentiometer	7	0.50	3.50
1000:1 Micro Metal Gearmotor	6	23.95	143.70
172:1 Metal Gearmotor 25Dx56L mm HP 6V	1	21.95	21.95
Breakout Board 9-DOF IMU BNO055	1	34.95	34.95
Black-Oxide Socket Head Screw, 2-56 Thread, 1/4" Long	1	6.43	6.43
18-8 Stainless Steel Phillips Flat, 2-56 Thread, 1/4" Long	1	3.94	3.94
Arduino Mega 2560	1	37.49	37.49
Breakout TB6612 1.2A Motor DVR	4	4.95	19.80
Heat-Set Insert for Plastics, 2-56 Thread, 0.115" Long	1	9.67	9.67
Ball Bearing, 5/16" OD, 68000 rpm Max Speed	2	15.35	30.70
Worm Gears (8 total)	1	56.00	56.00
CamBoard pico flexx	1	624.31	624.31
7.4 V 2800 mAh Battery	1	29.99	29.99
Capacitive Push Button	2	6.59	13.18
25D mm Metal Gearmotor Bracket Pair	1	7.45	7.45
Universal Aluminum Mounting Hub for 5mm Shaft, #4-40 Holes	1	7.49	7.49
Shaft Extender Reducer, 5mm Shaft, 4 mm Bore	1	37.74	37.74
440C Stainless/ISO 6 Ball Bearing, 4 mm Bore, 8 mm Outside Diam	2	13.98	27.96
303 ST. Steel Shaft, 4 mm Diam, 100 mm Long	1	5.06	5.06
Module 0.5, 30 Teeth Brass Spur Gear with Finished Bore	1	13.08	13.08
Module 0.5, 15 Teeth, 20 degree Pressure Angle, Brass Gear	1	9.75	9.75
3D Printed Palm and Fingers - ABS	1	63.96	63.96
3D Printed Wrist and Forearm - ABS	1	119.24	119.24
Food-Grade High-Temperature Silicone Rubber Sheet with Adhesive-Back, 6" x 6", 3/16" Thick, 40A Durometer	1	15.86	15.86
Custom PCB	1	5.60	5.60
		Total	**1,425.59**

Appendix C: Final Functionality Ratings

Device	Grips	Force (N)	Weight (g)	Wrist	Power	Battery Life (mAh)	Force Feedback	Vision
Axon Hook	1	111	N/A	Yes	Myo	N/A	No	No
Grip 5 Prehensor	1	N/A	259	No	Body	N/A	No	No
Michelangelo	7	70	420	Yes	Myo	1500	No	No
I-limb ultra	14	100	500	Yes	Myo	2000	No	No
BeBionic	14	140	690	Yes	Myo	2200	Yes	No
Ada Hand	5	49	380	No	Myo	N/A	No	No
Dexter	10	N/A	530	Yes	Neither	2800	Yes	Yes

These categories were ranked as follows:

- Grip: score based upon number of possible grips (for hooks number of grips was set as 1).
- Force: ranked based on maximum force during a power grip where 1 was the lowest and 6 is the highest.
- Weight: ranked where the lowest weight was a 6 and the highest was a 1.
- Wrist: 1 if there is a wrist and 0 if there is none.
- Power: 2 if myoelectric, 1 if body powered, zero if neither.
- Battery: longest battery life ranked the highest, body powered devices receive a 0.
- Force feedback: 1 if it's a capability, 0 if not.
- Visual: 1 if a capability.
- Functionality: sum of all classifiers where the highest score meant highest degree of functionality.

Device	Grip	Force	Weight	Wrist	Power	Battery	Force	Visual	Functionality
Axon Hook	1	3	7	1	2	0	0	0	14
Grip 5	1	1	6	0	1	0	0	0	9
Michelangelo	7	4	4	1	2	4	0	0	22
I-limb ultra	14	6	3	1	2	5	0	0	31
BeBionic	14	7	1	1	2	6	1	0	32
Ada Hand	5	2	5	0	2	0	0	0	14
Dexter	10	5	2	1	0	7	1	1	27